



**HAL**  
open science

## Effect of Fly Ash on microstructural and resistance characteristics of dredged sediment stabilized with lime and cement

Ana Paula Furlan, Andry Razakamanantsoa, Harifidy Ranaivomanana, Ouali Amiri, Daniel Levacher, Dimitri Deneele

### ► To cite this version:

Ana Paula Furlan, Andry Razakamanantsoa, Harifidy Ranaivomanana, Ouali Amiri, Daniel Levacher, et al.. Effect of Fly Ash on microstructural and resistance characteristics of dredged sediment stabilized with lime and cement. *Construction and Building Materials*, 2021, 272, pp.121637. 10.1016/j.conbuildmat.2020.121637 . hal-03031926

**HAL Id: hal-03031926**

**<https://hal.science/hal-03031926>**

Submitted on 23 Mar 2021

**HAL** is a multi-disciplinary open access archive for the deposit and dissemination of scientific research documents, whether they are published or not. The documents may come from teaching and research institutions in France or abroad, or from public or private research centers.

L'archive ouverte pluridisciplinaire **HAL**, est destinée au dépôt et à la diffusion de documents scientifiques de niveau recherche, publiés ou non, émanant des établissements d'enseignement et de recherche français ou étrangers, des laboratoires publics ou privés.



Distributed under a Creative Commons Attribution 4.0 International License

# Construction and Building Materials

## Effect of Fly Ash on microstructural and resistance characteristics of dredged sediment stabilized with lime and cement

--Manuscript Draft--

<b>Manuscript Number:</b>	CONBUILDMAT-D-20-06024R1
<b>Article Type:</b>	Research Paper
<b>Keywords:</b>	dredged sediment; Fly ash; Soil stabilization; mechanical resistance; microstructure
<b>Corresponding Author:</b>	Andry Rico RAZAKAMANANTSOA, Ph.D IFSTTAR Site de Nantes NANTES, BOUGUENAI FRANCE
<b>First Author:</b>	Ana Paula FURLAN, PhD
<b>Order of Authors:</b>	Ana Paula FURLAN, PhD Andry Rico RAZAKAMANANTSOA, Ph.D Harifidy RANAIVOMANANA, PhD Ouali AMIRI, PhD Daniel LEVACHER, PhD Dimitri DENELEE, PhD
<b>Abstract:</b>	Contribution of fly ash (FA) as a complementary additive for dredged sediment (DS) stabilization was studied. The study is focused on definition of an efficient combination(s) to raise the DS properties. FA with lime and cement with both was used. Then, micro and macroscale investigations was performed. Test results demonstrate that FA additions promoted nucleation, formation of cementitious compounds and fabric modifications in sediment. DS stabilized using FA component show lower shrinkage and higher mechanical resistance than that stabilized using conventional binders. FA is found to be efficient in sediment-lime and sediment-cement mixtures since it accelerates cementation and strength gain.

# 1 Effect of Fly Ash on microstructural and resistance characteristics of dredged 2 sediment stabilized with lime and cement

3  
4  
5  
6 4 Ana Paula FURLAN<sup>a,b</sup>, Andry RAZAKAMANANTSOA<sup>b</sup>, Harifidy RANAIVOMANANA<sup>c</sup>, Ouali AMIRI<sup>c</sup>,  
7 Daniel LEVACHER<sup>d</sup>, Dimitri DENELEE<sup>b,e</sup>  
8  
9

10  
11 <sup>a</sup> Dept. of Transportation Engineering, Sao Carlos School of Engineering, University of Sao Paulo, EESC, USP, Sao  
12 Carlos, Brazil  
13

14 <sup>b</sup> GERS-GIE, Université Gustave Eiffel, IFSTTAR, F-44344 Bouguenais, France

15  
16 <sup>c</sup> GEM, UMR, CNRS 6163, IUT de Saint-Nazaire, Rue Michel Ange 44600

17  
18 <sup>d</sup> M2C, UMR 6143, University Caen-Normandy, F-14000 Caen, France

19  
20 <sup>e</sup> Institut des Matériaux Jean Rouxel de Nantes, Université de Nantes, CNRS, 2 chemin de la Houssinière, BP  
21 32229, 44322 Nantes Cedex 3, France  
22

## 23 24 15 Highlights

- 25  
26 16 - FA acts as filler when incorporated with sediment at early age
- 27 17 - FA promotes nucleation, cementitious compound growth resulting in porosity refinement
- 28 18 - FA reduces shrinkage and increases strength gain of mixtures, regardless curing time
- 29 19 - The effectiveness of FA addition is confirmed when used with sediment-lime and sediment-cement

## 30 31 21 Abstract

32  
33  
34 22 This study deals with the definition of an efficient combination of fly ash (FA) with lime or cement and  
35 23 with both, to improve the dredged sediment (DS) properties. At early age, filler and nucleation effects  
36 24 of FA lead to a refinement of the microstructure in addition to the macro porosity reduction induced  
37 25 by lime and cement. At long term, the microstructure becomes denser due to the pozzolanic property  
38 26 of FA. At macroscale, DS stabilized using FA show lower shrinkage and higher mechanical resistance  
39 27 than that stabilized without FA, with more pronounced effects when FA is mixed with cement.  
40  
41  
42  
43  
44

45  
46 29 **Key words:** dredged sediment, fly ash, soil stabilization, mechanical resistance, microstructure  
47  
48  
49

## 50 31 1. Background

51  
52  
53 32 Selection of pavement materials is based on mechanical properties such as strength and stiffness. This  
54  
55 33 procedure is adequate in case of raw and inert materials are used. In stabilized materials, physical  
56  
57 34 changes and chemical reactions take place [1][2]. Therefore, it is important to identify modifications  
58  
59  
60  
61  
62  
63  
64  
65

1  
2 35 which occur at different levels, in order to determine how the action mechanisms of different additives  
3 36 affect soil resistance.  
4

5 37 Multiscale analysis leads to a comprehensive knowledge of improvement of stabilized soil using  
6  
7 38 hydraulic binders. In such a way that microscale analysis provides evidences of pozzolanic reactions,  
8  
9 39 cementing material formation and evolution of crystalline phases, and macroscale analysis explains  
10  
11 40 enhances in mechanical properties resulted from previous interaction highlighted at microscale level  
12  
13 41 [3][4].  
14  
15  
16

17 42 At present time, Portland cement and lime are considered as the most convenient stabilizers for soil  
18  
19 43 [2]. In soils stabilized using Portland cement, soil gradation changes since cement grains may fill a little  
20  
21 44 portion of the soil voids [5] [6]. Hence, cement hydration is responsible for the significant strength gain  
22  
23 45 over time. The mechanism of interaction between the different components can be explained as  
24  
25 46 follows: Portland cement hydrates using available water in the soil and form a stone-like material  
26  
27 47 [3][7].  
28  
29  
30  
31

32 48 Typical mineral components of Portland cement are calcium and silicon which are often in the form of  
33  
34 49 oxides, such as CaO, SiO<sub>2</sub>, Al<sub>2</sub>O<sub>3</sub> and FeO<sub>2</sub>. The main clinker constituents are tricalcium silicate (C<sub>3</sub>S),  
35  
36 50 dicalcium silicate (C<sub>2</sub>S), tricalcium aluminate (C<sub>3</sub>A), and calcium ferroaluminate (C<sub>4</sub>AF). To control  
37  
38 51 reaction rate, gypsum (C $\bar{S}$ H<sub>2</sub>) might be added to cement.  
39  
40  
41

42 52 It is known that the hydration of clinker constituents produces cementitious compounds such as  
43  
44 53 calcium silicate hydrates (C-S-H), calcium hydroxide (CH). In pre induction of hydration, cement reacts  
45  
46 54 with the available water and the most active phase C<sub>3</sub>S produces calcium ions and OH<sup>-</sup>, SO<sup>2-</sup><sub>4</sub>, K<sup>+</sup>, Na<sup>+</sup>.  
47  
48 55 In dormant stage, C<sub>3</sub>S hydration continues and C<sub>2</sub>S begins to be hydrated. CH separates from hydrolysis  
49  
50 56 of C<sub>3</sub>S and C<sub>2</sub>S and may precipitate into empty voids. Ettringite (Ett) also forms due to the reaction of  
51  
52 57 gypsum with C<sub>3</sub>S and C<sub>4</sub>AF [8].  
53  
54  
55

56  
57 58 Over time (at early stage), C-S-H crystalline phases form an acicular morphology which branch, forming  
58  
59 59 a honeycomb-shape structure. CH crystallizes in large crystals (~40μm), presenting hexagonal plate-  
60  
61  
62  
63  
64  
65

60 shape, depending on the produced lime amount in early stages and the available free space. Ettringite

61 crystalizes in a needle-shape, with length up to 10 $\mu$ m and diameter of 0.25  $\mu$ m, which does not branch.

62 All aforementioned phases and processes have been observed in cement-based materials, included in

63 soil-cement mixtures [3][7][9].

64 At microscale level, when cement is mixed with soil, the soil-cement mixture presents a significant gain

65 of mechanical strength. Soil-cement strength results from cementation bonds and pore space

66 reduction [10][11]. Accordingly, cementitious compounds fill up the pores and connect cement grains

67 resulting in the increase in intra-aggregate pore volume [12].

68 When lime is used in soil stabilization, soil fabric changes since lime addition induces cation exchanges

69 and generates flocculation/agglomeration mechanism, in short term. In other words, water dissolves

70 some constituents of lime (CaO, CaSO<sub>4</sub>, MgO and quartz) that react with soil and reduce double diffuse

71 layer (DDL), resulting in flocculation (agglomeration). This process reduces soil plasticity and improves

72 workability [13]. Over time, pozzolanic reactions take place at alkaline environment (pH=12), forming

73 cementitious compounds i.e. C-S-H and C-A-S-H, that are responsible for increasing of long-term

74 strength [3][10].

75 At microscale level, soil-lime strength gain is also explained based on the formation of cementitious

76 compounds from pozzolanic reactions. However, the increase of soil resistance generated by lime

77 addition is less significant than that observed in mixtures using cement; and the use of lime is

78 preferably recommended for clayey soils, in order to improve soil fabric, plasticity and workability [1]

79 [2][13]. It is also worth noting that the mechanical properties of lime-treated soils are affected by the

80 curing temperature. By studying the stiffness evolution of a silt soil stabilized with quicklime cured at

81 30 °C, Silva et al. [14] observed two different stages on the stiffness evolution suggesting the existence

82 of two different chemical phenomena involved. Evolution in the first stage seems to be mostly related

83 to the formation of calcium aluminate hydrates (CAH). However, the evolution in the second stage can

84 be more related to a structural rearrangement of CAH and the formation of calcium silicate hydrates

1  
2 85 (CSH). These two distinct stages involved in the evolution of elastic modulus (E) with time suggest the  
3 86 existence of two apparent activation energies (one for each process).

4  
5 87 To maximize the benefits of soil stabilization, a binary or ternary combination of hydraulic binder is  
6  
7 88 proposed. Most of the time, lime and cement combination is recommended. Lime-cement stabilization  
8  
9 89 combines workability enhancement from lime addition and resistance gain from cement addition. Both  
10  
11 90 additives may be mixed without disturbing their own action mechanism. However, multicomponent  
12  
13 91 mixed materials show differences in physical and chemical properties due to coexistence of cement  
14  
15 92 hydration and mineral admixtures, changing hydration kinetics process and microstructure formation  
16  
17 93 mechanisms [15]. According to [16] [17], the dosage of cement and the water content have a  
18  
19 94 significant impact on unconfined compression strength (UCS) values. By testing soil-cement mixtures  
20  
21 95 with dosage of cement between 10 and 13%, Ribeiro et al. [17] observed that UCS is always larger for  
22  
23 96 highest dosage of cement independently from the water to cement ratio, whereas independently from  
24  
25 97 the dosage of cement, there is a clear optimum water content providing the maximum UCS value.  
26  
27 98 Finally, compressive strength develops faster with time when larger water and cement ratios are  
28  
29 99 adopted. For treatment using lime, the effects of molding water content on UCS values seems to be  
30  
31 100 insignificant independently from the dosage of lime [18].  
32  
33  
34  
35  
36

37  
38  
39 101 For sustainable development purpose, the use of local soil, waste and industrial byproduct are  
40  
41 102 encouraged to supply earthwork and earthen structure [6][19][20]. Two well-known industrial  
42  
43 103 byproducts are often cited: bottom ash and fly ash. The benefits of use of bottom ash for road  
44  
45 104 construction was been recently studied by different authors [21], [22], [23]. On the other hand, the  
46  
47 105 use of fly ash still requires further investigation because different mechanisms of interaction need to  
48  
49 106 be clarified.  
50  
51  
52

53 107 Researches in concrete technology has demonstrated that fly ash (FA) improves mechanical properties  
54  
55 108 of concrete, reduces the costs of production and is ecologically beneficial. FA addition may enhance  
56  
57 109 durability of the matrix and reduces the loss of heat energy during cement hydration [15][24].  
58  
59  
60  
61  
62  
63  
64  
65

110 FA is a waste from coal-fired electrical power plants that is being studied as admixture in soil  
111 stabilization [6][12][20]. Commonly, FA is composed by calcium, silicon and aluminium. The main  
112 oxides are CaO, SiO<sub>2</sub> and Al<sub>2</sub>O<sub>3</sub>. Class C Fly ash contains about 20% of CaO which might induce cation  
113 exchanges, flocculation and pozzolanic reactions, resulting in strength gain. Aluminum rich  
114 composition of FA might promote a specific cementitious compounds formation, such as CAH and  
115 CASH [3][7][25].

116 In concrete, FA addition stimulates reaction rate of cement hydration, promotes nucleation and  
117 growth of cementitious compounds. However, FA may also retard the onset of acceleration (Stage III  
118 of hydration) because of (i) inhibition of CH precipitation due to the formation of water containing  
119 organic species and (b) slows formation of Ca rich surface layers on clinker phases, in the case of  
120 aluminum rich FA [26].

121 The effects of FA action on soils are then physical and chemical. At physical point of view, finer particles  
122 of FA would fill voids of soil particles. Chemically, pozzolanic products induced by FA presence would  
123 fill pores. Both effects reduce porosity so that microstructure becomes denser. As results, strength and  
124 stiffness are increased and compressibility is reduced [27].

125 Research findings suggest that FA disperses clusters of soil and strength development is controlled by  
126 FA hydration [20][28][29], leading to an analogy with the aforementioned processes in cement pastes.

127 It is worth noting that water content of the fly ash stabilized soil mixture affects the strength [30]. The  
128 maximum strength reached in soil-fly ash mixtures generally occurs at moisture contents below  
129 optimum moisture content for density. For silt and clay soils the optimum moisture content for  
130 strength is generally four to eight percent below optimum for maximum density while for granular  
131 soils the optimum moisture content for maximum strength is generally one to three percent below  
132 optimum moisture for density. Therefore, it is crucial that moisture content be controlled during  
133 construction. Initial water content significantly affects the efficiency of soil stabilization.

134 In soil stabilization, FA addition alone is not sufficient to significantly increase strength to the design  
135 allowable levels, then a combination with other additives is required [29]. Particular attention must be  
136 paid when FA is added to soil-cement mixture. FA may compete with cement for the water available  
137 in the soil. This competition may be detrimental to cement hydration and it is more problematic in soil-  
138 cement because of the typical low water and cement ratio (w/c).

139 Interestingly, in binary combination involving lime and FA, stabilized soils present some benefits  
140 resulting in strength gain. Notwithstanding, Sivapullaiah and Jha [29] indicate that there may be  
141 particular FA contents to find greater resistance in the short and long term, respectively. Low contents  
142 of FA increase strength in 28 days, whereas high contents of FA increase strength in 4-7 days. Generally,  
143 FA in soil-lime changes the rate of strength gain and not the strength itself. Therefore, FA content up  
144 to 15% is recommended. The effects of initial water content on the compressibility, strength,  
145 microstructure, and composition of a lean clay soil stabilized by compound calcium-based stabilizer  
146 composed of cement, lime and fly ash was investigated by Yin et al. [31]. It was observed that as the  
147 initial water content increases in the range studied (from 11 to 19%), both the compaction energy and  
148 the maximum compaction force decrease linearly and there are less soil aggregates or agglomerations,  
149 and a smaller proportion of large pores in the compacted mixture structure. In addition, for specimens  
150 cured with or without external water supply and under different compaction degrees, the variation  
151 law of the unconfined compressive strength with initial water content is different and the highest  
152 strength value is obtained at various initial water contents. Finally, with the increase of initial water  
153 content, the percentage of the oxygen element tends to increase in the reaction products of the  
154 calcium-based stabilizer, whereas the primary mineral composition of the soil-stabilizer mixture did  
155 not change notably.

156 Regarding the microstructure organization, Furlan et al. [6] demonstrate that FA addition refines the  
157 pore structure prior the development of pozzolanic reaction. This previous study demonstrates that  
158 FA can be used as soil stabilization additive. However, some question related to the reactivity of FA  
159 combined with other chemical additive requires further investigation. This paper aims to investigate



160 the contribution of FA in soil stabilization using hydraulic binders, with the purpose of finding: (i)  
161 technically compatible material options, (ii) rational use of waste and byproducts and (iii) optimized  
162 mix dosage.

## 163 **2. Experimental program**

164 Chemical stabilization of soils induces physicochemical changes of soils characteristics due to chemical  
165 interactions between additives and soil. These changes imply improvements in the mechanical  
166 behavior of the soil. Therefore, a multiscale analysis was selected in order to provide a holistic  
167 knowledge of the stabilization mechanisms.

168 If, on the one hand, microscopic analysis can show the new cementing products resulting from  
169 chemical reactions, on the other hand, it is worth quantifying their impacts on mechanical  
170 performance improvement of stabilized soils. Then, measurements of design and mechanical  
171 properties are necessary. Moreover, the combined use of these techniques allows to relate the  
172 changes in different scales, in order to highlight advantages and disadvantages of chemical  
173 stabilization.

174 Thus, the present experimental program aims to respond these questions, demonstrating the  
175 beneficial of using fly ash as a complementary additive in soil stabilization, indeed, when combined  
176 with conventional hydraulic binders.

177 In this study, dredged sediment from La Baule Le Pouliguen Harbor, France, and two cementitious  
178 additives were used. Fly ash was added to mixtures containing lime, cement and lime and cement.  
179 Only chemical stabilization was made (so without gradation correction) in order to find the best  
180 combination of additives to improve the characteristics of this dredged soil considered as waste,  
181 regarding economic and environmental aspects.

### 182 **2.1. Materials**

183 The geotechnical properties of the sediment were carried out in accordance with GTR guide [32]  
184 dedicated for embankment and pavement applications. Table 1 shows results of soil characterization  
185 based on results of maximum specific gravity, and organic material, pH and carbonates contents.

**Table 1.** Geotechnical properties of sediment

Parameters	Value
Sand fraction > 63 $\mu$ m (%)	23
Silt fraction - 2 to 63 $\mu$ m (%)	41
Clay fraction < 2 $\mu$ m (%)	36
Specific gravity (g/cm <sup>3</sup> )	2,66
Plasticity limit (%)	36.06
Liquidity Limit (%)	54.54
Plasticity Index	18.48
Organic matter content (%)	10.97
Carbonates content (%)	22.21
pH	8.5

187  
188 Proviacial® ST quicklime was added to the sediment soil. The quicklime was provided by LHOIST from  
189 Dugny-sur-Meuse, in Lorraine, France. This lime contains at least 90% of calcium oxide and at  
190 maximum 2% of magnesium oxide. The lime content added to soil was 2%.

191 Portland cement was a CEM II/B-LL 32,5R CE CP2 (French Standard) whose short-term resistance is  
192 32.5 MPa. Clinker content is between 65 and 79%, being its chemical constituents: tricalcium silicate  
193 (66%), dicalcium silicate (10%) and tricalcium aluminate (7%). Limestone is the main natural  
194 component of this cement, presenting a total organic material less than 0.20% in mass. The cement  
195 content added to soil was 7% of the dry mass of the sediment.

196 Sodeline® Fly ash is manufactured and was provided by the central Emile Huchet in Saint Avold, France.  
197 The main constituents of this fly ash are silicon dioxide (47.36%), aluminum oxide (21.63%) and calcium  
198 oxide (8.52%). It is important to point out that sulfur content (4.02%) is higher than the conventional  
199 ones. The fly ash content added to soil was 9%.

200 The particle size distribution of sediment, hydraulic binders and fly ash are summarized in Figure 1.

201 The particle size distributions help to understand the contribution of binders on the sediment particle  
202 arrangement. The particle size distributions were carried out with Malvern mastersizer.

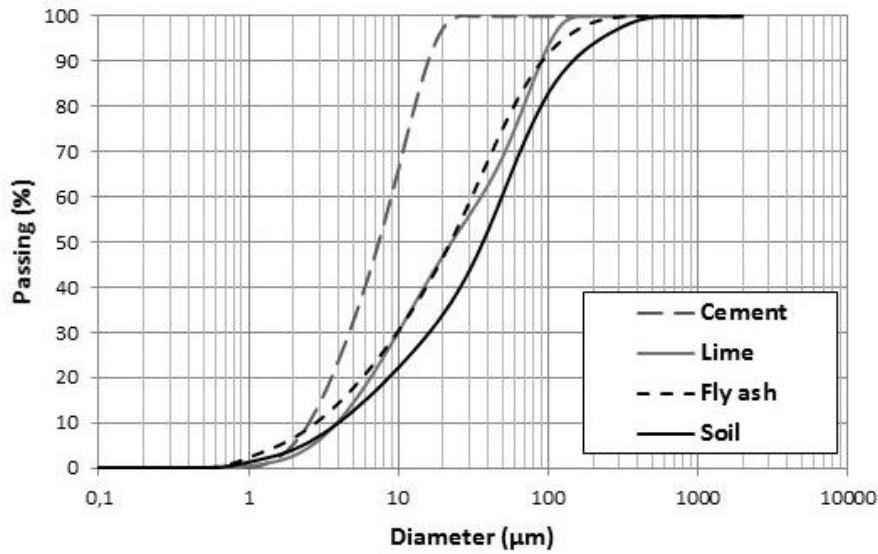


**Figure 1:** Grain size distribution of materials

Comparing the curves from Figure 1, it can be observed that the sediment is composed with coarsest material ( $D_{90}=150\ \mu\text{m}$ ), with particle diameters between 500 and  $1\ \mu\text{m}$ ; and cement is the finest binder compared to lime and FA ( $D_{90}=15\ \mu\text{m}$ ), with particle diameters between 10 and  $2\ \mu\text{m}$ , that is also the most uniform distribution. Particle-size distributions of lime and FA are quite similar ( $D_{90}=90\ \mu\text{m}$ ), with particle diameters between 200 and  $0.8\ \mu\text{m}$ .

## 2.2. Procedures of specimen preparation

Raw sediments have been oven-dried at  $50^{\circ}\text{C}$  for 48h prior to the treatment process. The sediment mixtures considered in this study are respectively formulated with 2% lime (S2L), 7% cement (S7C) or 2% lime and 7% cement (S2L7C). The percentages considered here correspond to the dry mass of sediment. A binary or ternary binder mixture has also been proposed for the mixture including fly ash (FA). The rate of fly ash addition, which is equal to 9%, represents the sum of the standard binder rates used, i.e. 2% lime and 7% cement: S2L9FA, S7C9FA, S2L7C9FA.

Proctor tests were performed according to French standard (NF P94-093) to get the optimum parameters of the mixtures, that is optimum water content and maximum dry density. All mixtures were prepared based on several precedent dosages [33]. In addition to mixture design, shrinkage tests

220 have been carried out to measure the effect of the binder on the volumetric strain of the compacted  
221 mixtures. Mixtures were compacted at their optimum characteristics in an oedometric cell of 101 mm  
222 in diameter and 7mm thick.

223 Specimens for UCS test were prepared according to Proctor optimum parameters. Mixing procedure  
224 considered the addition of extra amount of water due to the binder presence, in order to preserve the  
225 optimum Proctor parameters. Thus, water content was increased in 1% for each percentage of added  
226 lime, 0.4% for each percentage of added cement, and 0.1% for each percentage of added fly ash.

227 Before compaction, the mixtures using lime underwent a previous period of 2 hour in a closed recipient  
228 for the former reactions of lime and to avoid carbonation reactions. Cylindrical specimens  
229 (76mmx38mm) were statically compacted. After compaction, specimens were packed in plastic film,  
230 to prevent the loss of moisture during curing. Curing was made in a room at controlled temperature  
231 ( $20\pm 1^{\circ}\text{C}$ ) in different times, namely: 7, 28 and 90 days.

232 An extra specimen of each mixture was produced for the microstructure investigation. Cubic samples  
233 ( $10\text{mm}^3$ ) were sampled and freeze-dried from a compacted specimen at 7 and 28 days. To stop the  
234 hydration and chemical reactions of the binders, cubic samples had the water removed by sublimation.

### 235 **2.3. Methods**

236 Unconfined compression strength (UCS) tests were performed according to French standard (NF P94-  
237 420) under a constant strain rate of 1mm/min. After test, water content (w) was measured by oven  
238 drying method at  $105^{\circ}\text{C}$ . In total, 3 specimens were tested and all results represent the average value  
239 of UCS and w.

240 The volumetric deformation induced by shrinkage was followed until full stabilization within 9 days for  
241 all mixture. Volumetric deformation of all samples was monitored by means of a digital caliper.

242 Microscale analysis was based on X-ray diffraction (XRD) analyses, Scanning Electron Microscopy (SEM)  
243 observations and Mercury intrusion porosimetry (MIP) measurements.

244 XRD analyses were used not only to identify the crystallized component resulting from the hydration  
245 of cement and pozzolanic reactions but also to characterize sediment matrix. The XRD analyses were  
246 performed on powder using a Brucker diffractometer with a detector over the range  $5^{\circ}$ – $80^{\circ}2\theta$  using Cu-  
247  $K\alpha_1$  radiation ( $1.55\text{\AA}$ ). Diffractometer operated with input voltage of 30 kV and current of 10mA.  
248 Crystallography Open Database (COD) was used to identify constituents and new crystalline phases in  
249 the patterns.

250 SEM images were used to investigate the mineral phases resulting from the interaction between the  
251 sediment and the binder components. SEM observations were carried out using a FEI Inspect F-50 SEM  
252 instrument coupled to an energy dispersive X-ray analyzer (EDX). To improve the image quality,  
253 samples are coated with gold.

254 The impact of the mineral compound development on the sediment structure resulting from hydration  
255 mechanism of the binder mixture was followed by the pore distribution. The pore size distributions  
256 were plotted from MIP data obtained with Micromeritics Autopore IV.

### 257 **3. Results**

#### 258 **3.1. Microstructure investigation**

##### 259 **3.1.1. Microstructure investigation by XRD**

260 The main strength gain in chemical stabilized soil is mostly attributed to cementitious compounds  
261 formed from cement hydration and/or pozzolanic reactions. Figure 2 shows XRD patterns of all  
262 mixtures at 7 and 28 days. These patterns compare mixtures with original soil, in order to identify new  
263 crystalline phases addressed to chemical reactions. Different curing times are considered in attempt  
264 to evidence the formation and growth of cementitious compounds. New peaks in patterns confirmed  
265 not only the formation of cementitious compounds but also indicated the presence of non-hydrated  
266 materials.

267 In Figure 2, it is observed that untreated sediment presents quartz (Q), feldspar (F), calcium carbonate  
268 (C), Illite (I) and kaolinite (K) in its composition. Samples at 7 days (Figure 2a) showed the presence of

269 gypsum (S2L9FA), C<sub>2</sub>S (S2L7C and S2L7C9FA) and anhydrite (S7C). It may indicate (a) insufficient water  
1  
2 270 to hydrate the binders, (b) delay in cement hydration due to FA addition, (c) restricted water  
3  
4 271 availability of anhydrous grains surrounded by hydration products due to the formation of strong  
5  
6  
7 272 bounds between soil aggregates which can modify the porous structure and thus can slow down or  
8  
9 273 hinders the permeation and/or diffusion process of water, (d) a combination of previous assumptions.  
10  
11  
12 274 A remarkable peak of calcium carbonate (CaCO<sub>3</sub>) was particularly observed in S2L7C9FA at 7 days. The  
13  
14 275 occurrence of CaCO<sub>3</sub> was associated to the presence of limestone in the cement (CEM II) and  
15  
16 276 carbonates in the untreated sediment. The non-observation of such CaCO<sub>3</sub> peak in S7C or S2L7C could  
17  
18  
19 277 be explained by the heterogeneous distribution of binders in the sediment, the sediment itself and the  
20  
21 278 low percentage of cement used. Since the specimens have been kept packed during curing,  
22  
23  
24 279 carbonation reactions were disregarded.  
25  
26

27 280 Regarding hydration products, new peaks pointed out CH in S7C9FA, C-S-H in S2L and S2L7C, and  
28  
29 281 ettringite in S7C and S7C9FA. The mixture with S2L9FA presented CASH peak. Even though some  
30  
31 282 crystalized new phases from cement hydration have been identified, they did not occur in an evident  
32  
33  
34 283 way and this might be a consequence of the low water/cement ratio (w/c).  
35  
36

37 284  
38  
39  
40  
41  
42  
43  
44  
45  
46  
47  
48  
49  
50  
51  
52  
53  
54  
55  
56  
57  
58  
59  
60  
61  
62  
63  
64  
65

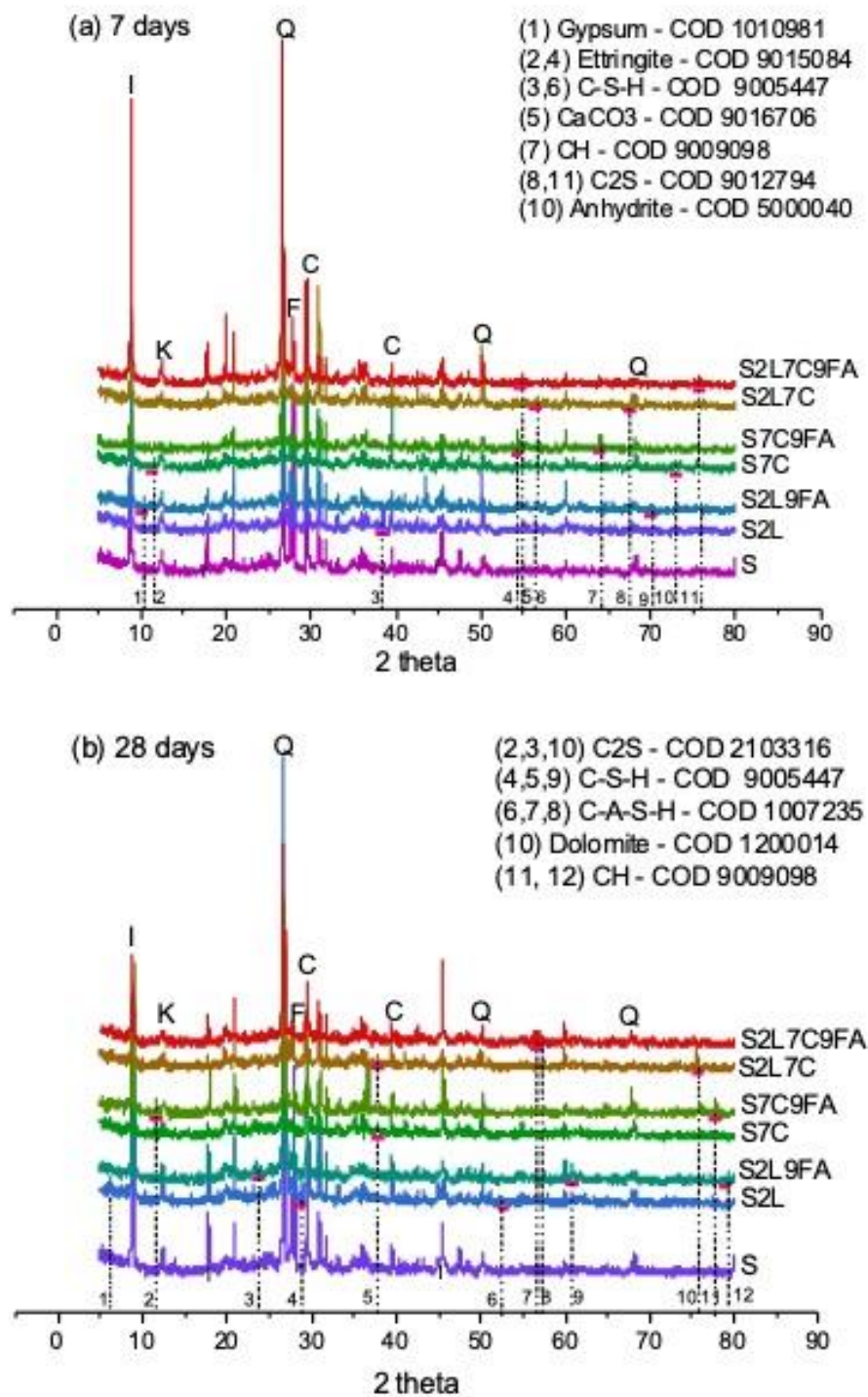


Figure 2: XRD results of mixtures at 7 days (a) and 28 days (b)

285  
286

287 Figure 2(b) shows the pattern of mixtures at 28 days. Belite is still identified in S7C9FA and S2L7C.  
 288 Other new peaks refer to C-S-H in S2L, S7C, S2L9FA and S2L7C, CH in S2L9FA and S7C9FA, and CASH in  
 289 S2L and S2L7C9FA. The presence of non-hydrated material suggests hydration delay or water

1  
2  
3  
4  
5  
6  
7  
8  
9  
10  
11  
12  
13  
14  
15  
16  
17  
18  
19  
20  
21  
22  
23  
24  
25  
26  
27  
28  
29  
30  
31  
32  
33  
34  
35  
36  
37  
38  
39  
40  
41  
42  
43  
44  
45  
46  
47  
48  
49  
50  
51  
52  
53  
54  
55  
56  
57  
58  
59  
60  
61  
62  
63  
64  
65

1  
2 291 insufficiency. This might be related to (i) lime addition, because the change of texture (agglomeration)  
3  
4 292 would interfere with the amount of available water for hydration, since water may be trapped in the  
5  
6 293 soil cluster; and/or (ii) FA addition, because water demand for FA is generally important due to its  
7  
8 294 appreciable porosity, it might create a competition for available water. Besides, it is important to  
9  
10 295 remember that cementitious compounds in early ages are poorly crystalized and they are not well  
11  
12 296 detected by diffractometer.

13  
14 297 Regarding cementitious compounds, one may observe that all treated samples had produced them at  
15  
16 298 28 days, unlike what happened at 7 days. Curing time was preponderant to development of  
17  
18 299 cementitious compounds, since time allows binders to hydrate according to their own reaction rates  
19  
20 300 (pozzolanic reactions) and allows also the transport of water necessary to the reactions of anhydrous  
21  
22 301 grains surrounded by hydration products. This implies that it would be recommended at least 28 days  
23  
24 302 to verify strength gains, at macroscale.

25  
26 303 Hydrated silicates exhibit different morphologies and it might be more problematic for chemically  
27  
28 304 stabilized soil due to the several factors, such as the type of additive, the low additive contents, the  
29  
30 305 low water content, the complexity of hydration mechanisms and cementitious material formation of  
31  
32 306 multicomponent mixed materials [15][25].  
33  
34 307

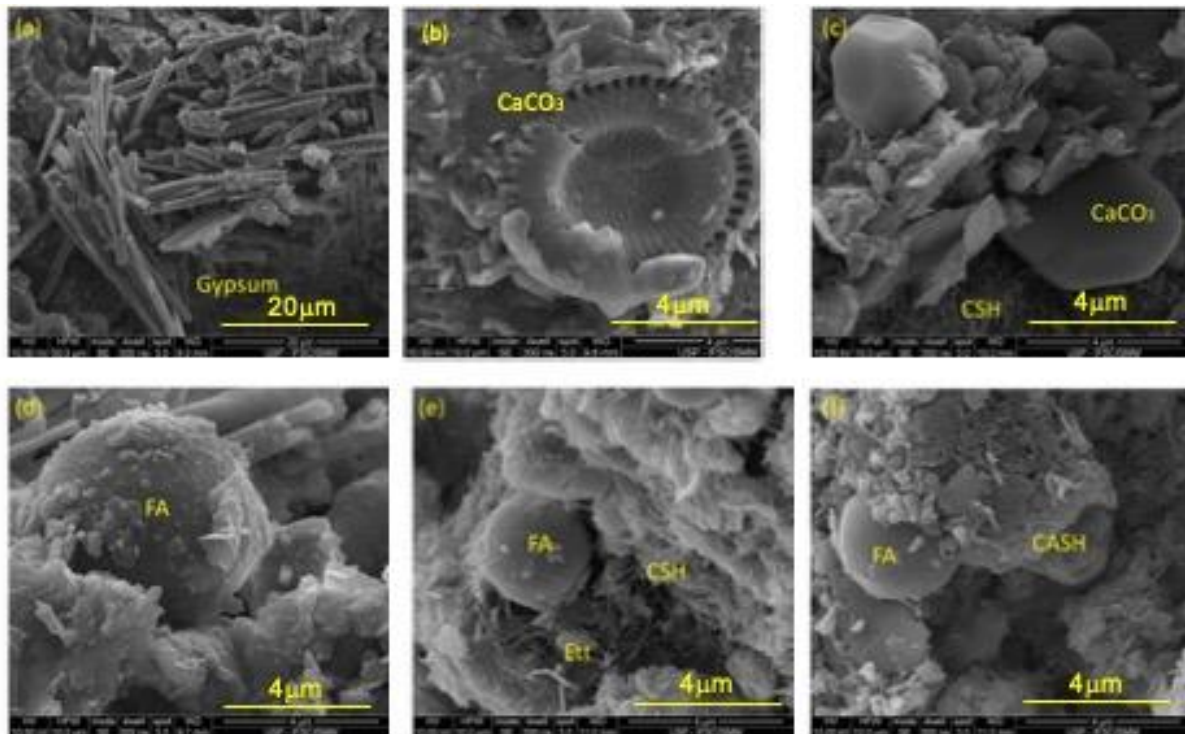
35  
36 308 In other words, since C-S-H are amorphous and/or poorly crystallized, it may be advisable to be careful  
37  
38 309 when reading XRD patterns because of the disturbing factors (producing a heterogeneous sample) and  
39  
40 310 to combine other microstructural data sources to help to support the results analyses.  
41  
42 311

### 43 312 **3.1.2. Microstructure observation by Scanning Electron Microscopy (SEM)**

44  
45 313 SEM images are often used to provide evidences of cementitious compounds development and  
46  
47 314 mixture changes. Firstly, Figure 3 attempts to demonstrate visually constituents and compounds,  
48  
49 315 which were previously identified in the mixtures using XRD tests (Figures 2 and 3). SEM Images are  
50  
51 316 presented in appropriate magnificence to highlight details of the materials. As it can be seen in figure  
52  
53 317



314 3, almost all compounds identified with the XRD patterns are observed and confirmed, such as gypsum,  
315  $\text{CaCO}_3$  (found in sediment and in mixtures with cement), hydrated silicates and FA as well.

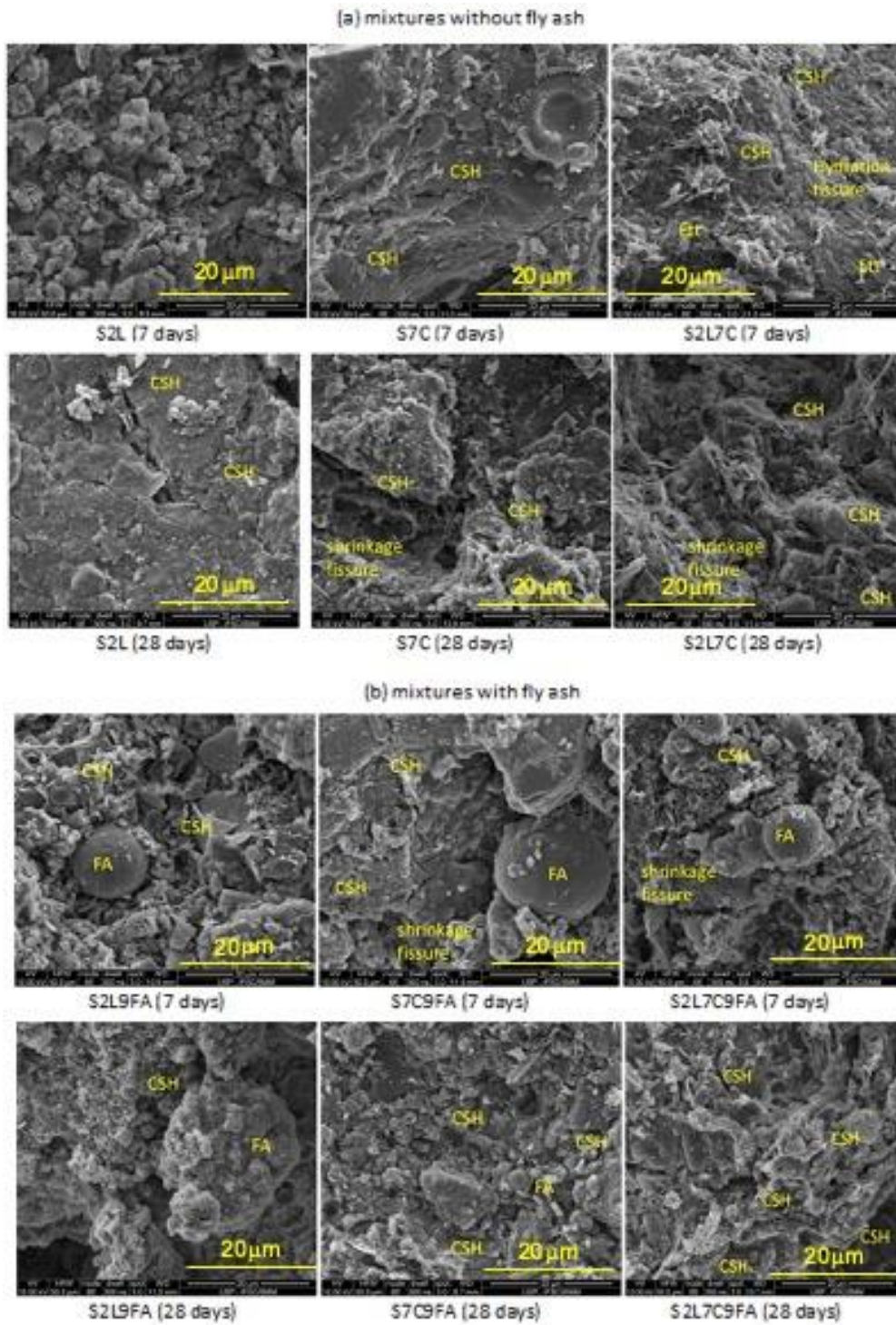


316  
317 **Figure 3:** Identification of constituents and cementitious compounds of mixtures from (a)S2L9FA-7d,  
318 (b) S7C, (c)S2L7C9FA – 7d, (d) S7L9FA – 7d, (e)S2L7C9FA-7d,(f) S2L9FA-28d

319 Secondly, Figures 4 shows SEM images obtained from sediment mixtures without and with FA (4a and  
320 4b), in order to observe structural changes and cementitious compound presence from 7 to 28 days.  
321 Figure 4(a) shows images from mixtures using conventional binders. Mixture with lime (S2L) at 7 days  
322 exhibits a flaked-like structure, as a result of cation exchange and flocculation mechanism. At 28 days,  
323 a block-like structure may be observed, indicating pozzolanic reactions, as demonstrated by  
324 identification of needle-shape C-S-H.

325 Regarding mixture with cement (S7C), block-like structure may be observed already at 7 days. Besides  
326 it might be identified the formation needle-shape C-S-H. Shrinkage fissure (due to cement hydration)  
327 are observed at 28 days.

328 The mixture with binary binder, lime and cement (S2L7C), exhibited a combination of the  
 329 aforementioned observations related to structure, i.e. flaked and block-like. Notwithstanding, in this  
 330 mixture, C-S-H and ettringite are identified and as well as some shrinkage fissures at 7 and 28 days.



331  
 332  
 333 **Figure 4:** SEM images from mixtures without FA (a) and with FA (b)

334 The observation of cementation products and the resulting block-like structure lead to infer some  
1  
2 335 increase in strength at macroscale, for instance. Again, that is in accordance with the assumption that  
3  
4 336 cementation enhances the mixture cohesion and controls strength gain of mixtures using cement [12].  
5  
6

7 337 Figure 4(b) presents images of binary and ternary mixtures using FA, in attempt to observe its effect  
8  
9 338 when combined with conventional binders. Generally, mixtures using FA revealed significant  
10  
11 339 occurrence of pozzolanic and hydration products. These phenomena are more effective surrounding  
12  
13 340 FA spheres. This finding is consistent to nucleation process and reaction stimulation reported in  
14  
15 341 technical literature [3][12][25].  
16  
17  
18

19 342 Concerning visual aspect, at 7 days, it can be observed that mixture with lime and FA shows a flaked-  
20  
21 343 like structure. At 28 days, mixture revealed a blocky structure. The change in structure is remarkable  
22  
23 344 and is attributed to the development of cementation between the soil clusters and also covering FA,  
24  
25 345 as seen in S2L9FA mixture at 28 days.  
26  
27  
28

29 346 For mixture with cement and FA (S7C9FA), blocky structure is observed at 7 and 28 days. C-S-H gel  
30  
31 347 covers the surface of soil and FA and shrinkage fissures were identified. For the mixture with lime,  
32  
33 348 cement and FA (S2L9FA), once again the flocculated structure was observed (at 7 days) as well as its  
34  
35 349 evolution to a blockier structure (at 28 days).  
36  
37  
38

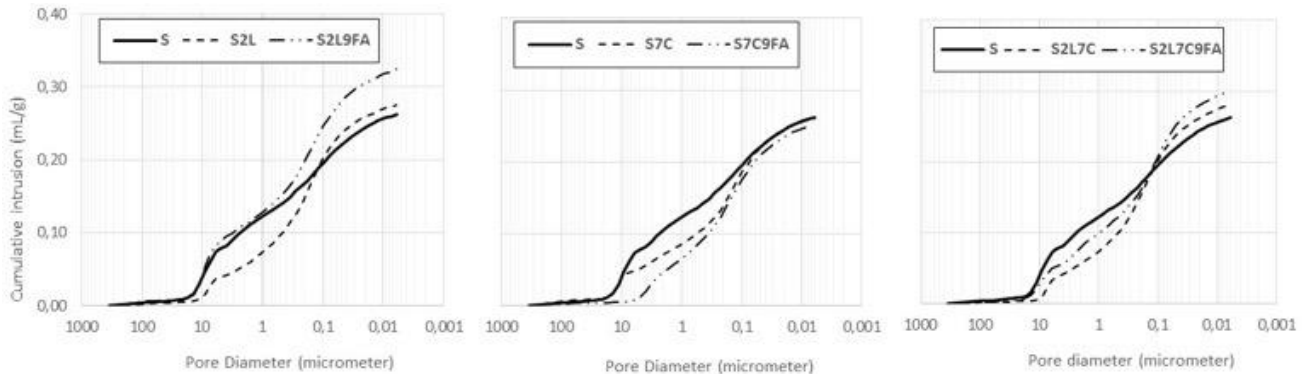
39 350 Cementitious compounds and hydration fissures seem to occur more frequently in mixtures using FA  
40  
41 351 for both curing time. The increase of CaO content due to addition of FA as long as the nucleation  
42  
43 352 process would promote formation of cementitious materials [3][4][26].  
44  
45  
46

### 47 353 **3.1.3 MIP results**

48  
49

50 354 The XRD patterns (Figure 2) showed the occurrence of cementation from new crystalline phases in the  
51  
52 355 mixtures such as hydrated silicates. The SEM images (Figures 4) confirmed the presence of the  
53  
54 356 cementitious compound and qualified the changes of the structure caused by the additives. MIP tests  
55  
56 357 were carried out, in attempt to clarify the mechanism of interaction between FA and conventional  
57  
58 358 binder which govern the alteration of sediment fabric.  
59  
60  
61  
62  
63  
64  
65

359 Figure 5 presents cumulative intrusion versus pore diameter curves. In general, additives reduced the  
 360 pore diameter of original soil. In mixtures S2L and S2L9FA, for large pores (from 10 to 0.1  $\mu\text{m}$ ), it is  
 361 observed that there are reductions of diameter of pore. Whereas, for small pores (from 0.1 to 0.001  
 362  $\mu\text{m}$ ) there is an increase of cumulative intrusion, i.e. an increase of percentage of small pores. Curves  
 363 are approximately parallels, but it can be seen that FA tends to change further large pores.



364  
 365  
 366 **Figure 5: Pore distributions of all mixtures (7 days)**

367 Mixtures S7C and S7C9FA presented significant changes mostly in large pores. This finding suggests  
 368 that changes in the pore distribution depend on the type and amount of binder added, and particularly  
 369 the gradation of binders.

370 Pore distributions revealed the soil fabric changes resulting from addition of binders. For instance, at  
 371 7 days, it is expected that:

372 (i) Lime generates a formation of aggregates/flocculates with finer pore width resulted from the  
 373 exothermic reaction which take place during lime hydration [10][34].

374 (ii) Cement hydration produces cementitious compounds that fill large pores and also causes  
 375 shrinkage reducing original soil pores diameter. No significant evolution of small pores domain is  
 376 observed for both treatments using lime and cement. This is due to the fact that small pores are  
 377 mainly associated with intra-aggregate porosity which is less affected by the treatment.

378 (iii) both lime and cement combine these two mentioned effects, and

379 (iv) in addition to the role of filler played by FA, it also promotes nucleation and formation of  
 1  
 2 380 cementitious compounds around FA, increasing the percentage of small pores of the original soil  
 3  
 4 381 [12].  
 5

6  
 7 382 Since total pore volume (i.e. the highest cumulative intrusion value) is an indicator of material  
 8  
 9 383 densification, one could assume that, at macroscale, the resistance of mixtures using FA would be  
 10  
 11 384 higher than that of mixtures without FA. Nevertheless, accordingly [28], cementation controls  
 12  
 13 385 predominantly the resistance development of soil-cement mixtures.  
 14  
 15

### 16 386 3.2. Macroscale analysis

17  
 18  
 19  
 20 387 Macroscale analysis was done in two steps. The first consisted of immediate property assessment of  
 21  
 22 388 the mixtures based on Proctor, shrinkage, and UCS test results. The latter was based on UCS results  
 23  
 24 389 throughout curing time. First and second steps focused on distinguishing the filler effect from curing  
 25  
 26 390 effect, respectively, in an attempt to remark the most adequate stabilization process, in terms of  
 27  
 28  
 29 391 additive content and strength gain.  
 30  
 31

#### 32 392 3.2.1. Design parameters and immediate strength

33  
 34  
 35 393 Binder addition and content may change soil gradation. Since additives are finer than the soil (Figure  
 36  
 37 394 1), they shall fill partially empty voids of soil and increase the initial strength values, due to the filler  
 38  
 39 395 effect. Table 2 present design parameters and immediate strength. Comparing to untreated sediment,  
 40  
 41 396 it is observed that binder addition promoted (a) the reduction of maximum dry densities ( $\rho_{dmax}$ ) and  
 42  
 43 397 the increase of optimum water content ( $w_{opt}$ ), (b) the reduction of the volumetric variation ( $dv$ ) and  
 44  
 45 398 (c) the increase of immediate strength ( $UCS_{0d}$ ). Nevertheless, the intensity of changes depends on the  
 46  
 47 399 type and the content of binder.  
 48  
 49  
 50  
 51

52 400 **Table 2.** Design parameters and immediate strength

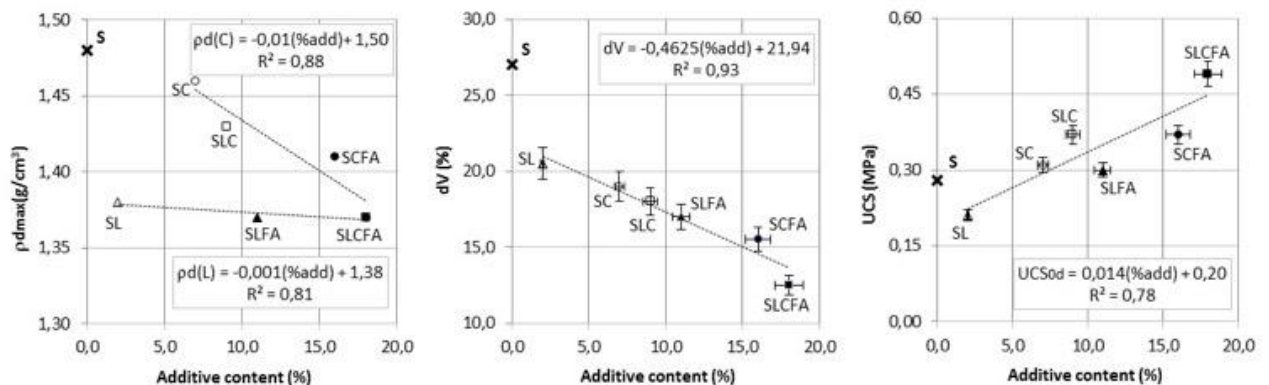
Type of mixture	Legend	% filler	Proctor Parameters		Shrinkage Parameters			UCS <sub>0d</sub> (MPa)
			w <sub>opt</sub> (%)	ρ <sub>dmax</sub> (g/cm <sup>3</sup> )	Time (days)	dv (%)	dv/T (%/hours)	
Soil	S	0,0	27.8	1.48	3,0	27.0	0.44	0.28

Soil+ 2% lime	S2L	2.0	32.2	1.38	2.6	20.5	0.50	0.21
Soil+ 2% lime + 9% fly ash	S2L9FA	11.0	32.0	1.37	2.8	17.0	0.39	0.30
Soil+ 7% cement	S7C	7.0	28.1	1.46	2.4	19.0	0.32	0.31
Soil+ 7% cement + 9% FA	S7C9FA	16.0	30.3	1.41	3.0	15.5	0.33	0.37
Soil+ 2% lime+ 7% cement	S2L7C	9.0	30.7	1.43	2.2	18.0	0.25	0.37
Soil+ 2% lime+ 7% cement+9% FA	S2L7C9FA	18.0	31.6	1.37	2.0	12.5	0.17	0.49

To illustrate filler effect, Figure 6 shows correlations between Proctor and shrinkage parameters, and immediate UCS values in function of additive content. Figure 6(a) shows that the reduction of  $p_{dmax}$  is a result of the increase of binder content, but this behavior depends on the type of binder considered. It is observed that the evolution of the  $p_{dmax}$  follow a linear regression law with high degree of accuracy ( $R^2$ ).  $R^2$  values for mixtures containing lime (L) and cement (C) are 0.81 and 0.88, respectively. FA addition reduced  $p_{dmax}$  in mixtures with cement. In mixtures with lime this behavior was not observed.

Linear law demonstrates that cement addition reduces maximum dry density less than lime addition. Both curves converge to the  $p_{dmax}$  value of the SLCFA mixture, which was the minimum one.

Volumetric deformation is often consequence of shrinkage which occurs in cemented materials due to the water consumption for clinker component, generating fissures. Shrinkage test reports the variation of volume ( $dV$ ) that a soil-cement may present and gives an idea about material durability in dosage phase. Figure 6(b) shows a strong correlation between  $dV$  and additive content ( $R^2=0.93$ ), indicating that  $dV$  decreases with increasing additive content. In other words, partial filling of the voids would inhibit shrinkage.



418

**Figure 6: Immediate Properties and characteristics of mixtures**

1  
2  
3  
4  
5  
6  
7  
8  
9  
10  
11  
12  
13  
14  
15  
16  
17  
18  
19  
20  
21  
22  
23  
24  
25  
26  
27  
28  
29  
30  
31  
32  
33  
34  
35  
36  
37  
38  
39  
40  
41  
42  
43  
44  
45  
46  
47  
48  
49  
50  
51  
52  
53  
54  
55  
56  
57  
58  
59  
60  
61  
62  
63  
64  
65

419 It would be reasonable to indicate the addition of inactive fillers in order to reduce shrinkage in soil-  
420 cement type mixtures. Figure 6(b) led to infer that FA plays this role in this phase, because its addition  
421 in the mixtures further reduced dV. In mixtures without FA, the reduction of dV was approximately  
422 equals to 30% in relation to untreated soil. When FA was added, this reduction was about 40% for SL  
423 and SC mixtures, and 55% for SLC mixture.

424 Regarding the filler effect on immediate strength, Figure 6(c) shows a good correlation ( $R^2=0.79$ )  
425 between additive content and UCS of the mixtures, where the higher the additive content the greater  
426 the UCS<sub>0d</sub>. It is important to point out that immediate UCS<sub>0d</sub> of SL mixture was lower than the  
427 untreated sediment. This behavior is attributed to flocculation reactions of lime that increase of voids  
428 in the mixture, decreasing  $p_{dmax}$  and increasing water content (as seen in Table 2).

429 It is worth emphasizing that the combination of additives changes gradation of untreated sediment.  
430 As additives are finer than the sediment soil, they may fill empty voids, increasing the sediment  
431 strength. As a rule, the initial strength values gradually improve as binder percentages increase.

432 In spite of the good correlation between immediate UCS and additive content, the strength gain may  
433 be also related to the type of additive, or combination between them, since the greatest immediate  
434 UCS were observed in mixtures SLC, SCFA and SLCFA. The common point of these mixtures is the  
435 presence of cement associated to other(s) additive(s). It seems to be a contribution of additive  
436 gradations to the particle size arrangement of mixtures, resulting in the increase of their immediate  
437 UCS. Immediate UCS is a reference point that might lead to dosage optimization attempts. Accordingly,  
438 from this point on, it shall be observed the strength gain over time due to chemical reactions.

**3.2.2. UCS and water content results over time**

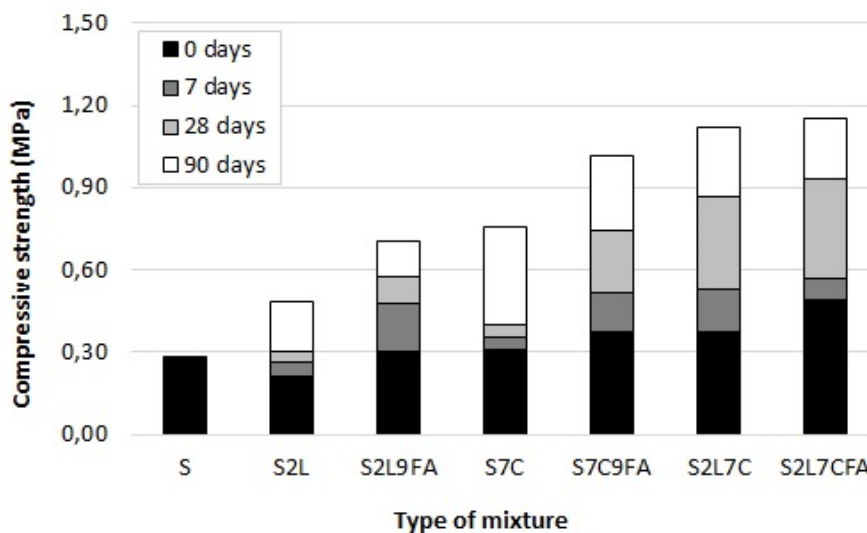
440 In order to highlight the effects of additives on the mechanical resistance of mixtures, Figure 7 presents  
441 the kinetics of the UCS over time. Regarding compressive strength values (UCS), one may observe that  
442 additives increased initial property of untreated sediment (0,27 MPa), even though some mixtures

443 required more time to present significant strength gains, such as mixture S2L that presented reduction  
 1  
 2 444 of UCS value at 7 days. All other additives combination increased UCS values and these increases are  
 3  
 4 445 more expressive when FA is added.  
 5  
 6

7 446 From 0 to 7 days, the strength gain of S2L and S7C was about 0.05 MPa that represents respectively  
 8  
 9 447 20% and 16% of their initial UCS values (0.21 and 0.31 MPa). For conventional binders, the mixture  
 10  
 11 448 with lime and cement (S2L7C) had the higher strength gain (~0.15 MPa), that is 40% of its initial  
 12  
 13 449 strength (0.37 MPa).  
 14  
 15

16  
 17 450 For mixtures containing FA, strength gains were in average of 0.15 MPa. It is worth emphasizing the  
 18  
 19 451 strength gain of the mixture S2L9FA that was about 70%. In contrast, the strength gain at 7 days of the  
 20  
 21 452 mixture S2L7C9FA was the lowest one (0.10MPa) that represents about 20% of initial UCS value.  
 22  
 23

24  
 25 453 At 28 days, the UCS value of S2L was 0.31 MPa, S7C was 0.40 MPa, and S2L7C was 0.87 MPa. From 7  
 26  
 27 454 to 28 days, the gain of UCS remains about 0.05 MPa for S2L and S7C. Interestingly, FA addition  
 28  
 29 455 doubled the strength gains in these mixtures. The faster strength gain was also observed by Kang et al.  
 30  
 31 456 [27].  
 32  
 33  
 34  
 35



457  
 458 **Figure 7: UCS over time**  
 459

459 For the mixture S2L7C9, the strength gain was 0.35 MPa. In this case, FA addition did significantly not  
 58  
 59 460 increase strength gain of SLC mixture. In general, mixtures with FA presented the higher UCS values.  
 60  
 61  
 62  
 63  
 64  
 65



1  
2  
3  
4  
5  
6  
7  
8  
9  
10  
11  
12  
13  
14  
15  
16  
17  
18  
19  
20  
21  
22  
23  
24  
25  
26  
27  
28  
29  
30  
31  
32  
33  
34  
35  
36  
37  
38  
39  
40  
41  
42  
43  
44  
45  
46  
47  
48  
49  
50  
51  
52  
53  
54  
55  
56  
57  
58  
59  
60  
61  
62  
63  
64  
65

461 In order to observe the tendency of strength evolution, Figure 7 also presents UCS at 90 days. As it can  
462 be noticed, UCS values continued increasing, with emphasis on the highest strength gains of mixture  
463 S7C and S2L. Another point to remark is that mixtures using FA showed slower strength gains compared  
464 to mixtures with conventional binders, unlike what was observed for other curing time (7 and 28 days),  
465 suggesting a deceleration of these gains at 90 days.

466 UCS Kinetics confirmed the additive mechanism-based assumptions. Regarding mixture with lime,  
467 cation exchanges and flocculation did not improve soil resistance. Over time, pozzolanic reactions were  
468 not effective to increase significantly the strength even in long term (from 28 days). In the mixture with  
469 cement, the occurrence of cementitious compounds increased strength at early age (7 days).  
470 Interestingly, it continued to increase up 90 days but at lower intensities, in contrast to expectations  
471 of fast reacting cements. This delay is probably associated to the salt presence and organic matter in  
472 the marine sediment that alters the kinetics of hydration cement, as mentioned by Horpibulsuk et al.  
473 [35].

474 On the other hand, FA addition has led to the higher strength gains in all tested mixtures. This  
475 observation is consistent with the hypotheses of nucleation and growth of cementitious materials  
476 promoted by FA [15][26][27], which here were observed and discussed based on the results of  
477 microscale test (Figures 2 to 4).

478 Assuming that the gain of resistance over time results from the cementing products of the additive  
479 components [28], it is also necessary to understand how the hydric state of the mixtures evolves.  
480 Figure 8 presents the evolution of water content over time. The plotted curves indicate that water  
481 content reduces over time and the intervals of variation are significant over long periods, as can be  
482 seen for all mixtures using cement.

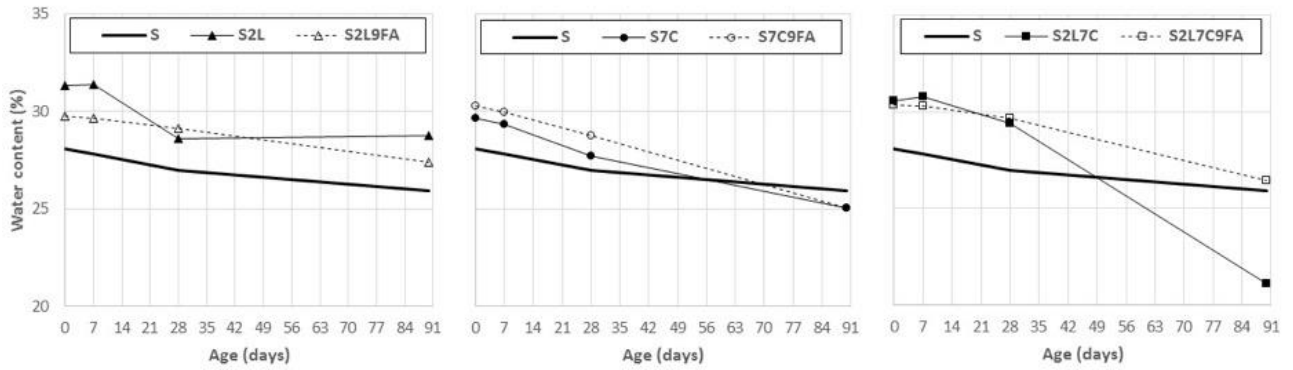


**Figure 8:** Variation of water content over time

In early age (7 days), water contents change slightly, maintaining practically the initial values, i.e. close to the  $w_{opt}$  (Table 4). However, for intermediary age (28 days), these changes evidence the reduction of water content, the average reduction was 5%. For longer period (90 days), the average reduction of water content is 12%, except for SLC, which was 31%.

FA addition also alters hydric conditions of stabilized mixtures over time but at lower intensity. As a rule, one may suppose that the greater the decrease in moisture content the greater the gain in resistance. This hypothesis is true since water is consumed in formation and/or crystallization of cementing products, becoming the structure denser and more resistant than the original soil.

#### 4. Discussion

The decision for a given product takes into account technical, economic and environmental parameters. This study has shown that combining FA with stabilized soil with lime and cement (or both) is promising because of the FA action mechanisms promoted an acceleration of strength gain regardless of the curing time. Besides, mixtures using FA have always shown higher resistance, either through physical interactions or chemical reactions. These findings support technically the choice for combining FA with chemical soil stabilization using conventional binders.

For instance, UCS value at 90 days of mixture using cement (S7C) is compatible with that of the mixture using cement and FA (S7C9FA) at 28 days, or with mixture using lime and FA (S2L9FA) at 90 days. These mechanical compatibilities indicate alternative material options that might save time and economy,

1  
2 504 since it is possible to select mixtures that present greater resistance ahead of time, use cheaper  
3 additives or smaller quantities of conventional binders.

4  
5 506 These benefits have a positive impact on environmental indicators because they promote the rational  
6 use of waste and byproducts (marine sediment and fly ash). In this sense, it is worth mentioning that  
7 507 the mixture with lime, cement and FA (S2L7C9FA) presented resistance compatible with the mixture  
8 without FA (SLC), leading to question the advantages of this mixture (S2L7C9FA) as well as to think  
9 508 alternatively about the possibility of reducing the cement content in order to optimize the mixture  
10 design in terms of economic and environmental.  
11  
12  
13  
14  
15  
16  
17  
18  
19

## 20 512 **5. Conclusions**

21  
22 513 The effects of FA addition on microstructural and resistance characteristics of mixtures stabilized with  
23 conventional binders were investigated. From this study the conclusions are made focusing the  
24 interrelations between microstructural and macrostructural analyses.  
25  
26  
27  
28  
29

30 516 Regarding microstructural analyses, it was identified new crystalline phases in DRX patterns.  
31 Cementitious materials, such as ettringite, portlandite and hydrated silicates, are produced over time  
32 by cement hydration and pozzolanic reactions. The occurrence of these products depends on the  
33 curing time due to particular binder reaction rate. These findings are supported by SEM images, that  
34 confirmed the presence of hydrated silicates in different morphologies (gel, acicular C-S-H for  
35 instance), mainly in mixtures using FA. The SEM images also show physical modification of the soil  
36 fabric over time, which was also confirmed by analysis of pore distributions. The results of the pore  
37 distribution measurements show a structural densification of the sediment matrix at early age,  
38 demonstrating the contribution of finer gradations of the additives on the sediment pore  
39 rearrangement, i.e. filler effect.  
40  
41  
42  
43  
44  
45  
46  
47  
48  
49  
50  
51  
52  
53

54 526 Macroscale analyses led also to observe a prevalent filler effect on gain of immediate resistance and  
55 reduction of volumetric variation by shrinkage (dV). These physical responses are especially  
56 remarkable in mixtures using FA. These findings led to recommend more studies in dosage parameters  
57  
58  
59  
60  
61  
62  
63  
64  
65

529 and properties in order to identify the best combination of binder blend for chemical stabilization  
1  
2 530 purposes and to optimize the mixture design with several binders, i.e. the choice and the content of  
3  
4 531 binder(s). UCS values increase and water contents decrease over curing time, with emphasis on the  
5  
6  
7 532 significant contribution of FA to the better mechanical performance. Based on microstructural analysis,  
8  
9 533 it can be stated that available water was consumed for cementing and pozzolanic reactions over time.  
10

## 11 534 **6. Acknowledgement**

12  
13  
14  
15 535 The authors are very thankful of the research team of University Gustave Eiffel and University of  
16  
17 536 Nantes for laboratory experiments and technical supports.  
18  
19

## 20 537 **7. Funding Source**

21  
22  
23 538 This work was financially supported by CAPES-PRINT in the framework of Post doctoral fellowship ref.  
24  
25 539 88887.371953/2019-00.  
26  
27

## 28 540 **8. References**

- 29  
30 541 [1] Rajasekaran, G. (2005) Sulphate attack and ettringite formation in the lime and cement stabilized marine  
31 542 clays. *Ocean Eng.* 32, pp. 1133-1159. [DOI:10.1016/j.oceaneng.2004.08.012](https://doi.org/10.1016/j.oceaneng.2004.08.012).  
32  
33 543 [2] Puppala, A.J. (2016) Advances in ground modification with chemical additives: From theory to practice,  
34 544 *Transportation Geotechnics*, 9, pp. 123-138. [DOI: 10.1016/j.trgeo.2016.08.004](https://doi.org/10.1016/j.trgeo.2016.08.004).  
35  
36 545 [3] Solanki, P., Zaman, M. (2012) Microstructural and mineralogical characterization of clay stabilized using  
37 546 calcium-based stabilizers. *Scanning Eletro Microscopy*, Ed. Dr. Viacheslav Kazmiruk, Intech, pp. 772-798.  
38 547 [DOI: 10.5772/34176](https://doi.org/10.5772/34176).  
39  
40 548 [4] Horpibulsuk, S. (2012) Strength and microstructure of cement stabilized clay. *Scanning Eletron Microscopy*,  
41 549 Ed. Dr. Viacheslav Kazmiruk, Intech, pp. 440-480. [DOI: 10.5772/35225](https://doi.org/10.5772/35225).  
42  
43 550 [5] Simoni, J.P.S.C. (2019). Contribution regarding the design and the mechanical behavior of soil-aggregate-  
44 551 cement mixture for pavement course. Dissertation (Master degree). 130p. Sao Carlos School of Engineering,  
45 552 University of Sao Paulo (*in Portuguese*).  
46  
47 553 [6] Furlan, A.P., Razakamanantsoa A., Ranaivomanana H., Levacher D., Katsumi T. (2018) Shear strength  
48 554 performance of marine sediments stabilized using cement, lime and fly ash. *V. 184*, pp. 454-463.  
49 555 [DOI: 10.1016/j.conbuildmat.2018.06.231](https://doi.org/10.1016/j.conbuildmat.2018.06.231).  
50  
51 556 [7] Chew, S.H., Kamruzzaman, A.H.M., Lee, F.H. (2004) Physicochemical and engineering behavior of cement  
52 557 treated clays. *J. Geotech. Eng.*, V. 130 (7) pp 696-706. [DOI: 10.1061/\(ASCE\)1090-024130:7\(696\)](https://doi.org/10.1061/(ASCE)1090-024130:7(696)).  
53  
54 558 [8] G. Ye. (2003) Experimental study and numerical simulation of the development of the microstructure and  
55 559 permeability if cementitious materials. PhD thesis. Delft University of Technology.  
56  
57 560 [9] Franus, W., Panek, R., Wdowin, M. (2015) SEM Investigation of Microstructures in Hydration Products of  
58 561 Portland Cement. In: Polychroniadis E., Oral A., Ozer M. (eds) 2nd International Multidisciplinary Microscopy and  
59 562 Microanalysis Congress. Springer Proceedings in Physics, vol 164, Springer, Cham.  
60  
61  
62  
63  
64  
65

- 563 [10] Lemaire, K. Deneele, D. Bonnet, S. Legret, M. (2013) Effects of lime and cement treatment on the  
1 564 physicochemical, microstructural and mechanical characteristics of a plastic silt, *Engineering Geology*. 166,  
2 565 pp. 255–261. DOI: [10.1016/j.enggeo.2013.09.012](https://doi.org/10.1016/j.enggeo.2013.09.012).
- 3 566 [11] Ranaivomanana H., Razakamanantsoa A., Amiri O. (2018) Effects of Cement Treatment on Microstructural,  
4 567 Hydraulic, and Mechanical Properties of Compacted Soils: Characterization and Modeling. *Int. J. Geomech.*, 2018,  
5 568 18(9): 04018106. DOI: [10.1061/\(ASCE\)GM.1943-5622.0001248](https://doi.org/10.1061/(ASCE)GM.1943-5622.0001248).
- 7 569 [12] Horpibulsuk, S. Rachan, R., Raksachon, Y. (2009) Role of fly ash on strength and microstructure development  
8 570 in blended cement stabilized silty clay. *Soils and Foundation*. Volume 48, Issue 1, pp. 85-98.  
9 571 DOI: [10.3208/sandf.49.85](https://doi.org/10.3208/sandf.49.85).
- 11 572 [13] Consoli, N.C., Lopes Jr., L.S., Heineck, K.S. (2009) Key parameters for strength control of lime stabilized soils.  
12 573 *J. Mater. Civ. Eng.*, V.21 (5), pp. 210-216. DOI: [10.1061/\(ASCE\)0899-1561\(2009\)21:5\(210\)](https://doi.org/10.1061/(ASCE)0899-1561(2009)21:5(210))
- 14 574 [14] Silva, J., Azenha, M., Gomes Correia, A., François, B., (2018). Two staged kinetics of moduli evolution with  
15 575 time of a lime treated soil under different curing temperatures. *Transportation Geotechnics*. Volume 17, Part A,  
16 576 pp. 133-140. DOI: [10.1016/j.trgeo.2018.09.013](https://doi.org/10.1016/j.trgeo.2018.09.013).
- 17 577 [15] Yin, B., Kang, T., Kang, J., Chen, Y., Wu, L., Du, M. (2018) Investigation of the hydration kinetics and  
18 578 microstructure formation mechanism of fresh fly ash cemented filling materials based on hydration heat and  
19 579 volume resistivity characteristics. *Applied Clay Science*, V. 166, pp.146-158. DOI: [10.1016/j.clay.2018.09.019](https://doi.org/10.1016/j.clay.2018.09.019).
- 21 580 [16] Consoli, N.C., Rosa, A.R., Cruz, R.C., Dalla Rosa, A., (2011). Water content, porosity and cement content as  
22 581 parameters controlling strength of artificially cemented silty soil. *Engineering geology*. Volume 122, (3-4), pp.  
23 582 328-333. DOI: [10.1016/j.enggeo.2011.05.017](https://doi.org/10.1016/j.enggeo.2011.05.017).
- 25 583 [17] Ribeiro, D., Néri, R., Cardoso, R., (2016). Influence of water content in the UCS of soil-cement mixtures for  
26 584 different cement dosages. *Procedia Engineering*. Volume 143, (3-4), pp. 59-66. DOI:  
27 585 [10.1016/j.proeng.2016.06.008](https://doi.org/10.1016/j.proeng.2016.06.008).
- 29 586 [18] Consoli, N.C., Prietto, P.D.M., Lopes Jr., L.S., Winter, D., (2014). Control factors for the long term compressive  
30 587 strength of lime treated sandy clay soil. *Transportation Geotechnics*. Volume 1 (3), pp. 129-136. DOI:  
31 588 [10.1016/j.trgeo.2014.07.005](https://doi.org/10.1016/j.trgeo.2014.07.005).
- 32 589 [19] Siham, K. Fabrice, B. Edine A.N., Degrugilliers, P. (2008) Marine dredged sediments as new materials  
33 590 resource for road construction. *Waste Management*, 28 - 5, pp. 919-928. DOI: [10.1016/j.wasman.2007.03.027](https://doi.org/10.1016/j.wasman.2007.03.027).
- 35 591 [20] Phetchuay, C., Horpibulsuk, S., Arulrajah, A., Suksiripattanapong, C., Udomchai, A. (2016) Strength  
36 592 development in soft marine clay stabilized by fly ash and calcium carbide residue based geopolymer. *Applied*  
37 593 *Clay Science* 127-128, pp. 134-142. DOI: [10.1016/j.clay.2016.04.005](https://doi.org/10.1016/j.clay.2016.04.005).
- 39 594 [21] Hung Le, N., Razakamanantsoa, A., Nguyen M., Phan V.T., Dao P., Nguyen D.H. (2018). Evaluation of  
40 595 physicochemical and hydromechanical properties of MSWI bottom ash for road construction. V.80, pp. 168-174.  
41 596 DOI: [10.1016/j.wasman.2018.09.007](https://doi.org/10.1016/j.wasman.2018.09.007)
- 43 597 [22] Thuy Minh Nguyen, T., Rabbanifar, S., Brake, A. N., Qian, Q., Kibodeaux, K., Crochet, H.E., Oruji, S, Whitt, R.,  
44 598 Farrow, J., Belaire, B., Bernazzani, B., Jao, M., (2018).Stabilization of silty clayey dredged material. *Journal of*  
45 599 *Material in Civil Engineering*. Volume 30 (9), DOI: [10.1061/ASCEMT.1943-5533.0002391](https://doi.org/10.1061/ASCEMT.1943-5533.0002391)
- 46 600 [23] Yoobanpot, N., Jamsawang, P., Poorahong, H., Jongpradist, P., Likitlersuang, S., (2020). Multiscale laboratory  
47 601 investigation of the mechanical and microstructural properties of dredged sediments stabilized with cement and  
48 602 fly ash. *Engineering geology*. Volume 267. DOI: [10.1016/j.enggeo.2020.105491](https://doi.org/10.1016/j.enggeo.2020.105491).
- 50 603 [24] Lee, C.Y., Lee, H.K., Lee, K.M. (2003) Strength and microstructural characteristics of chemically activated fly  
51 604 ash–cement systems. *Cement and Concrete Research*, 33, pp. 425-431. DOI: [10.1016/S0008-8846\(02\)00973-0](https://doi.org/10.1016/S0008-8846(02)00973-0).
- 53 605 [25] Fernandez, R., Ruiz, A.I., Cuevas, J. (2016) Formation of C-A-S-H phases from the interaction between  
54 606 concrete or cement and bentonite. *Clay Minerals*, V. 51, pp. 223-235. DOI:[10.1180/claymin.2016.051.2.09](https://doi.org/10.1180/claymin.2016.051.2.09).
- 56 607 [26] Biernacki, J.J., Williams, P.J., Stutzman, P.E. (2001) Kinetics of reaction of calcium hydroxide and fly ash. *ACI*  
57 608 *Materials Journal* 98(4), pp. 340-349.
- 58 609 [27] Kang, X., Kang, G.C., Chang, K.T., Ge L. (2015) Chemically Stabilized Soft Clays for Road-Base Construction. *J.*  
59 610 *Mater. Civil. Eng. ASCE*, 27(7) ASCE4 (ASCE) MT.1943-5533.0001156.

611 [28] Horpibulsuk, S., Rachan, R., Chinkulkijniwat, A., Raksachon Y., Suddeepong, A. (2010) Analysis of strength  
1 612 development in cementstabilized silty clay form microstructural considerations. *Constr. Build. Mater.* 24, pp.  
2 613 2011–21. [DOI:10.1016/j.conbuildmat.2010.03.01](https://doi.org/10.1016/j.conbuildmat.2010.03.01).

3 614 [29] Sivapullaiah, P.V., Jha, A.K. (2014) Gypsum induced strength behaviour of fly ash-lime stabilized expansive  
4 615 soil. *Geotech Geol Eng* 32: 1261. [DOI : 10.1007/s10706-014-9799-7](https://doi.org/10.1007/s10706-014-9799-7).

6 616 [30] American Coal Ash Association. (2003). Fly ash facts for highway engineers. Technical Report (FHWA-IF-03-  
7 617 019).

8 618 [31] Yin, C., Zhang, W., Jiang, X., Huang, Z., (2018). Effects of Initial Water Content on Microstructure and  
9 619 Mechanical Properties of Lean Clay Soil Stabilized by Compound Calcium-Based Stabilizer. *Materials*. Volume  
10 620 11(10) : 1933. DOI: 10.3390/ma11101933

12 621 [32] Guide des Terrassements Routier (GTR), Réalisation des remblais et des couches de forme, in: Technical  
13 622 guide, Fascicule 1, Principe généraux, 2nd Ed, SETRA – LCPC, D 9233-2, 2000, 221p.

15 623 [33] Liang, Y. (2012) Co-valorisation de sédiments et de sols fins par apport de liants et de fibres, PhD thesis, U.  
16 624 Caen – Normandie.

18 625 [34] Cuisinier O., Auriol, J.C. Borgne, T., Deneele, D. (2011) Microstructure and hydraulic conductivity of a  
19 626 compacted lime-treated soil, *Engineering Geology*, 123, 187–193. [DOI: 10.1016/j.enggeo.2011.07.010](https://doi.org/10.1016/j.enggeo.2011.07.010).

20 627 [35] Horpibulsuk, S., Phojan, W., Suddeepong, A., Chinkulkijniwat, A., Liu, M.D. (2012) Strength development in  
21 628 blended cement admixed saline clay. *Applied Clay Science* 55, pp. 44-52. [DOI: 10.1016/j.clay.2011.10.003](https://doi.org/10.1016/j.clay.2011.10.003)

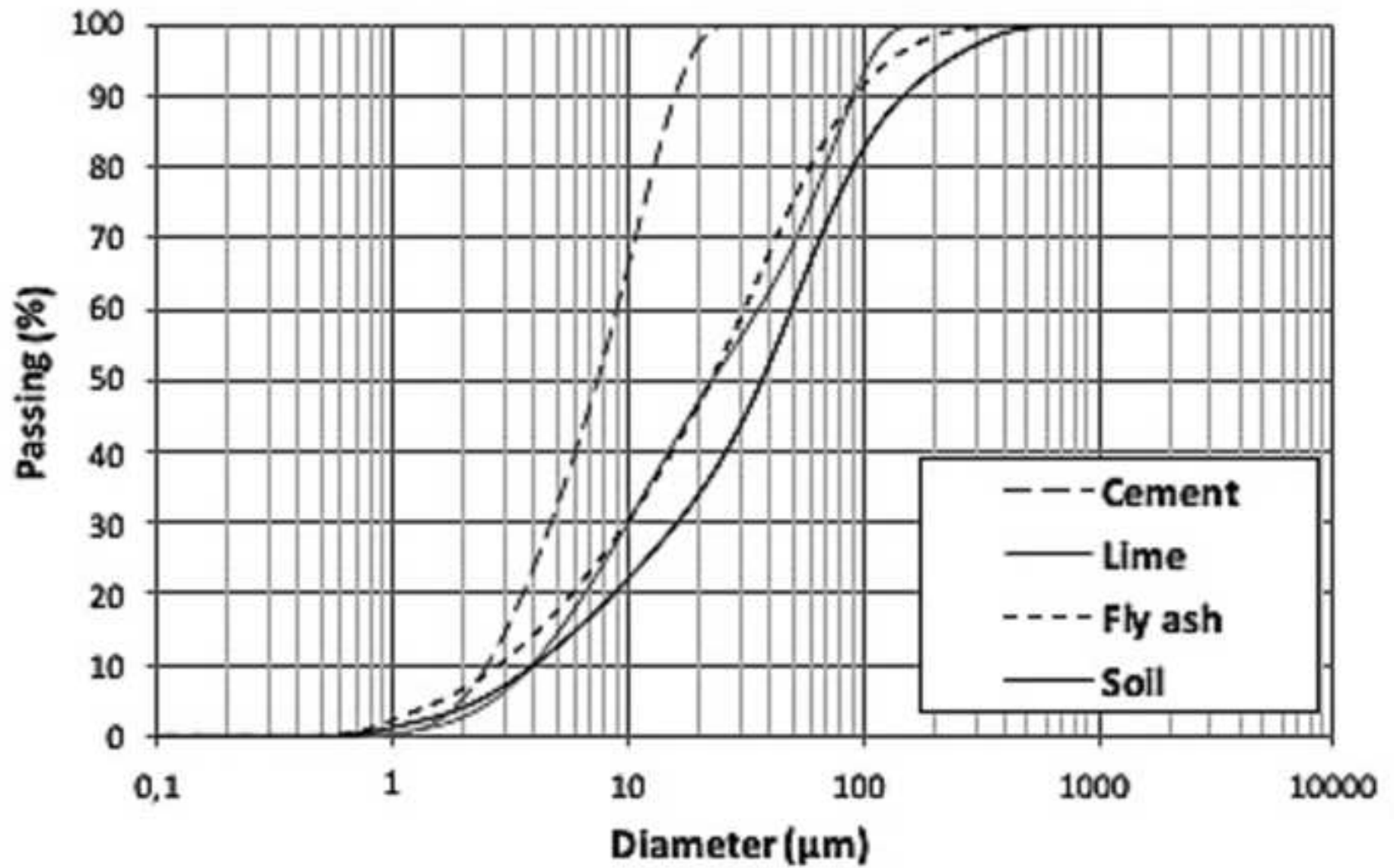
23 629  
24  
25 630  
26 631  
27  
28  
29  
30  
31  
32  
33  
34  
35  
36  
37  
38  
39  
40  
41  
42  
43  
44  
45  
46  
47  
48  
49  
50  
51  
52  
53  
54  
55  
56  
57  
58  
59  
60  
61  
62  
63  
64  
65

Parameters	Value
Sand fraction > 63 $\mu$ m (%)	23
Silt fraction - 2 to 63 $\mu$ m(%)	41
Clay fraction < 2 $\mu$ m (%)	36
Specific gravity (g/cm <sup>3</sup> )	2.66
Plasticity limit (%)	36.06
Liquidity Limit (%)	54.54
Plasticity Index	18.48
Organic matter content (%)	10.97
Carbonates content (%)	22.21
pH	8.5

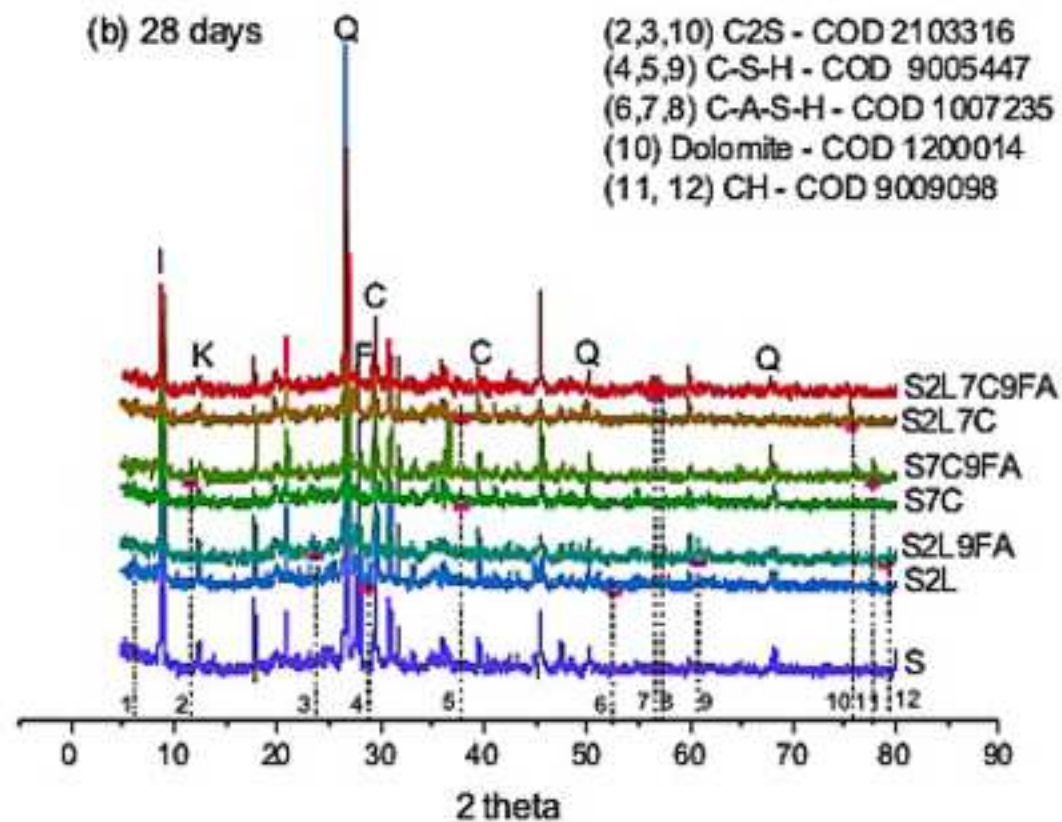
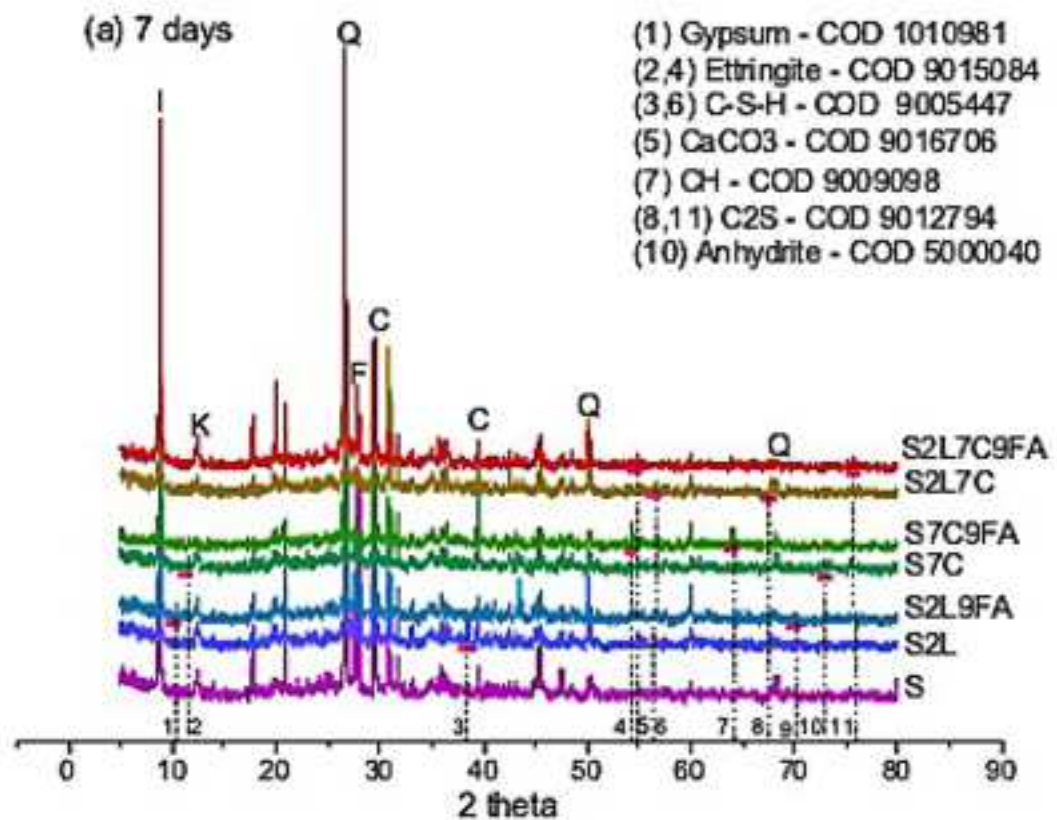
Table 1: Geotechnical properties of sediment

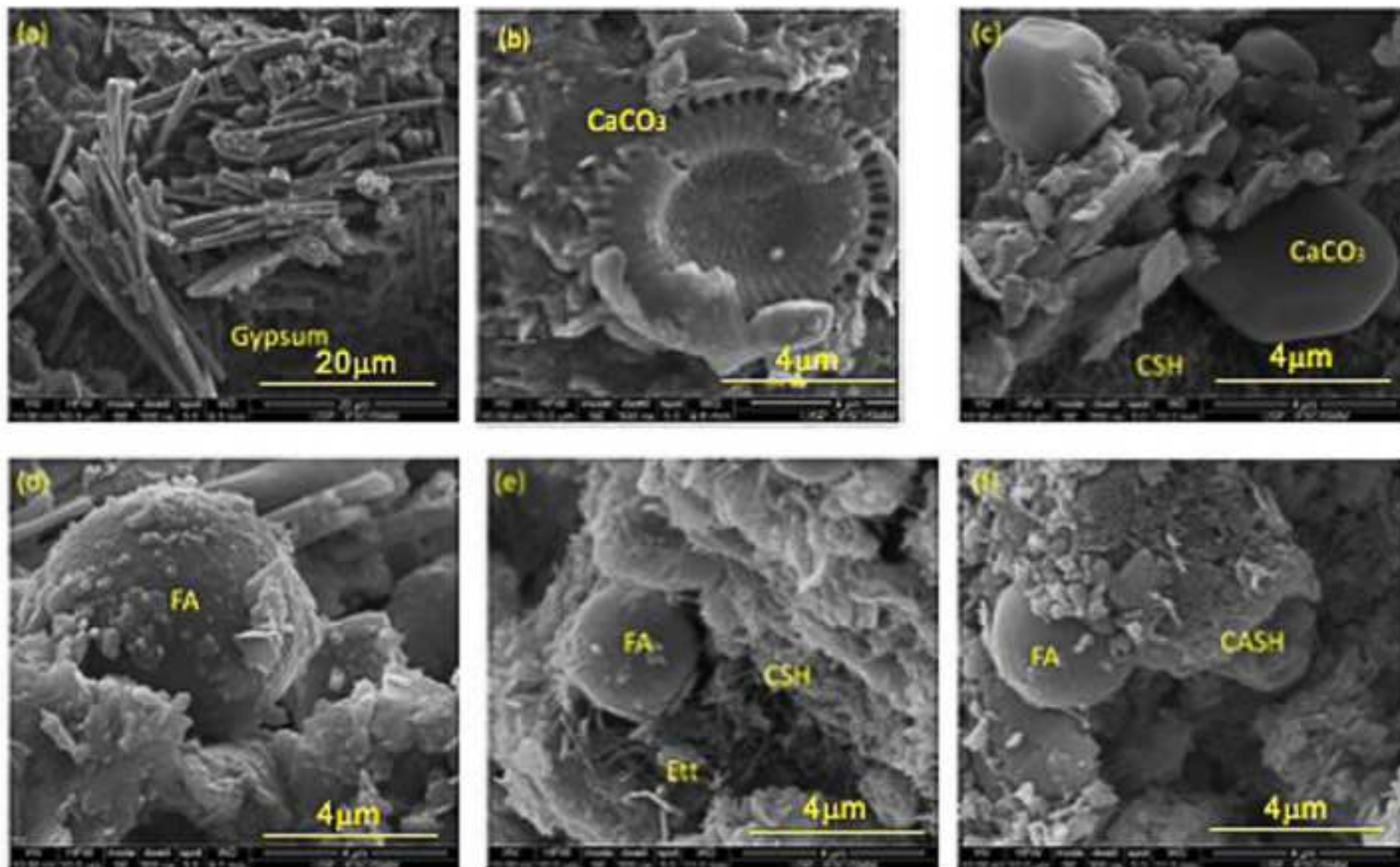
Type of mixture	Legend	% filler	Proctor Parameters		Shrinkage Parameters			UCS <sub>0d</sub> (MPa)
			W <sub>opt</sub> (%)	$\rho_{dmax}$ (g/cm <sup>3</sup> )	Time (days)	dv (%)	dv/T (%/hours)	
Soil	S	0,0	27.8	1.48	3,0	27.0	0.44	0.28
Soil+ 2% lime	S2L	2.0	32.2	1.38	2.6	20.5	0.50	0.21
Soil+ 2% lime + 9% fly ash	S2L9FA	11.0	32.0	1.37	2.8	17.0	0.39	0.30
Soil+ 7% cement	S7C	7.0	28.1	1.46	2.4	19.0	0.32	0.31
Soil+ 7% cement + 9% FA	S7C9FA	16.0	30.3	1.41	3.0	15.5	0.33	0.37
Soil+ 2% lime+ 7% cement	S2L7C	9.0	30.7	1.43	2.2	18.0	0.25	0.37
Soil+ 2% lime+ 7% cement+9% FA	S2L7C9FA	18.0	31.6	1.37	2.0	12.5	0.17	0.49

Table 2: Design parameters and immediate strength

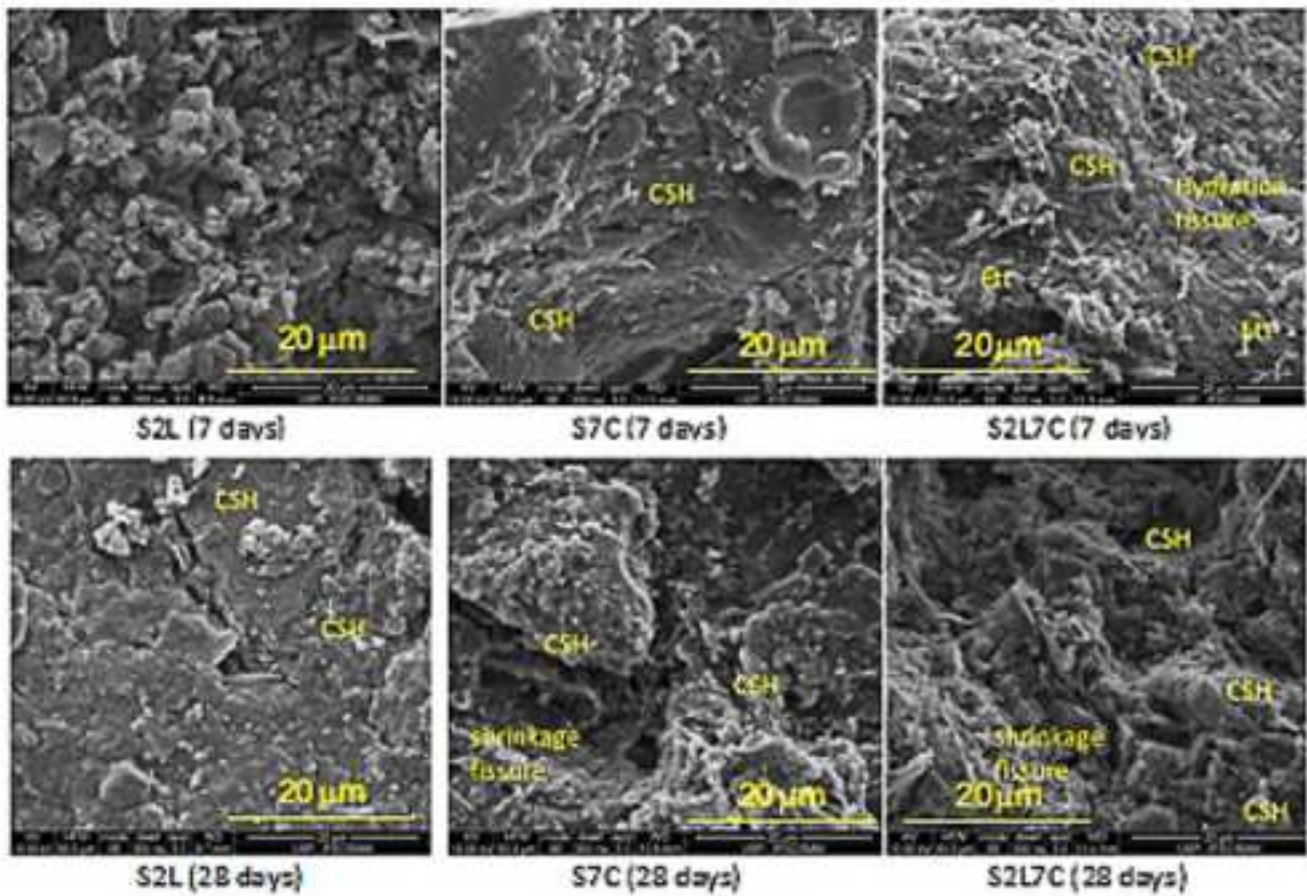




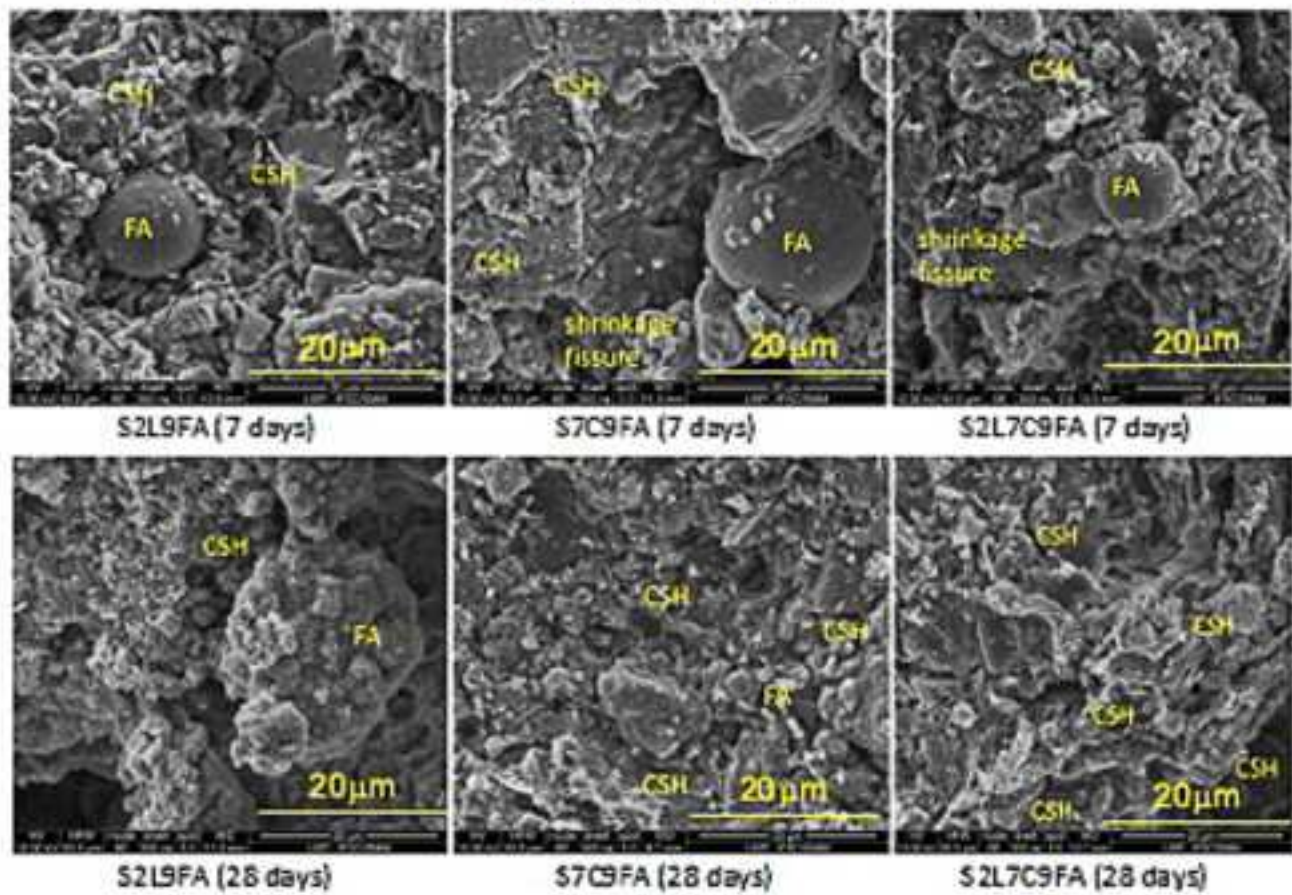


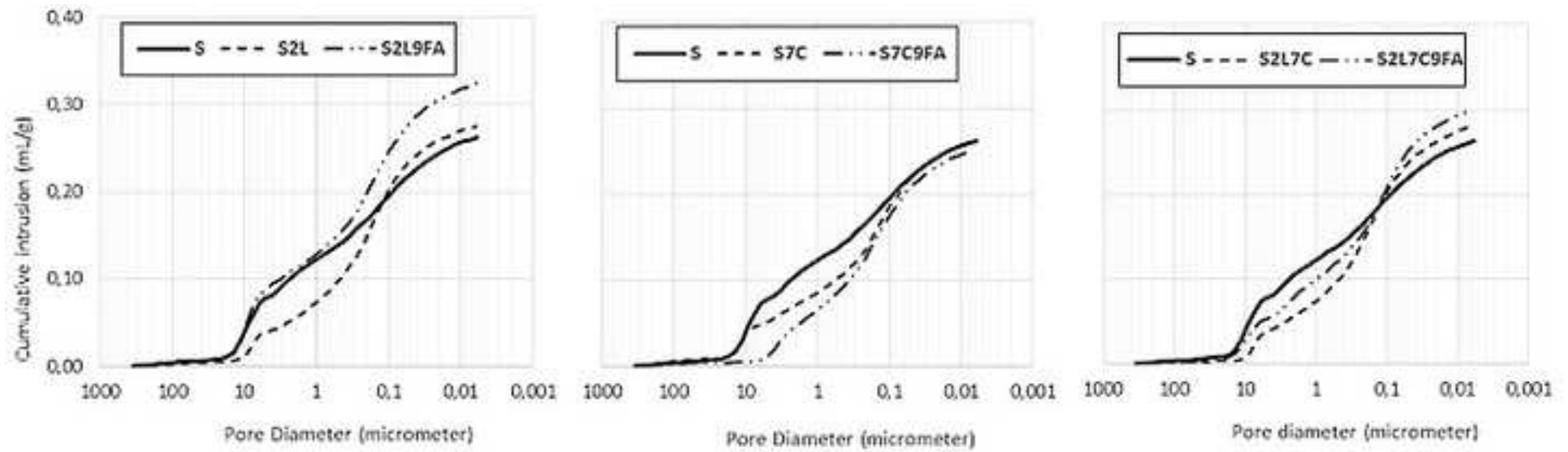


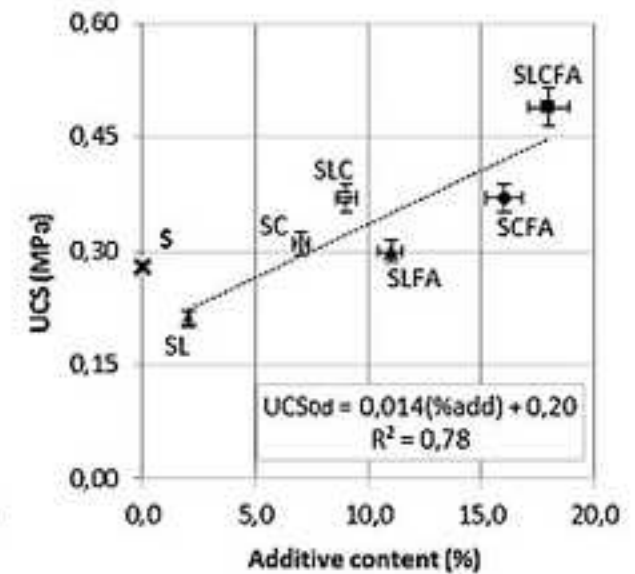
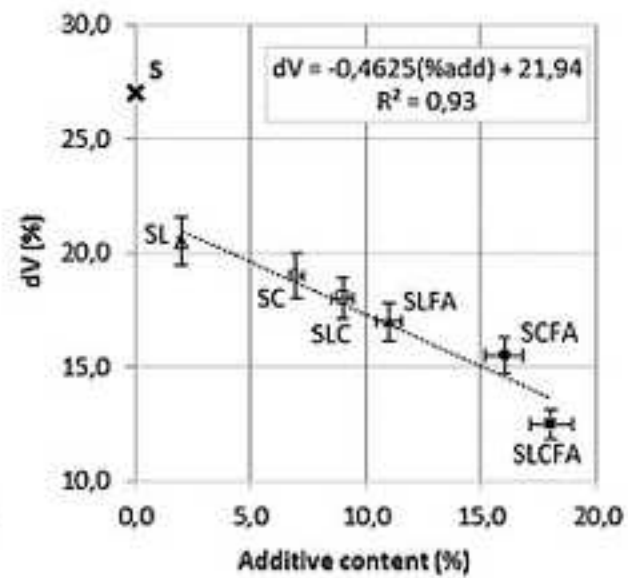
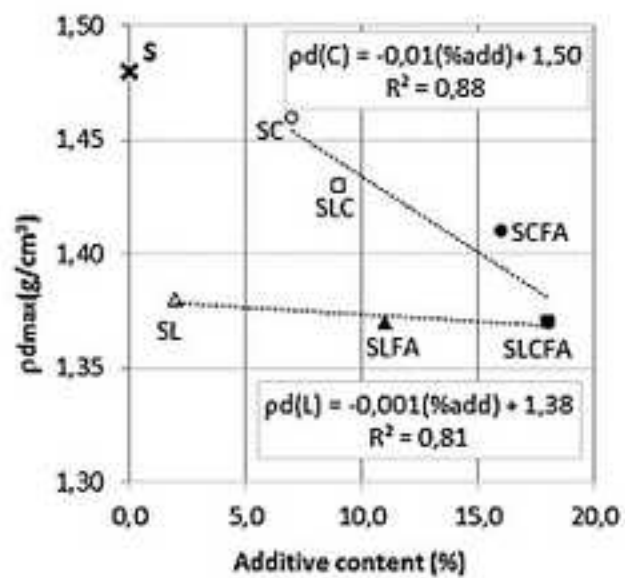
(a) mixtures without fly ash

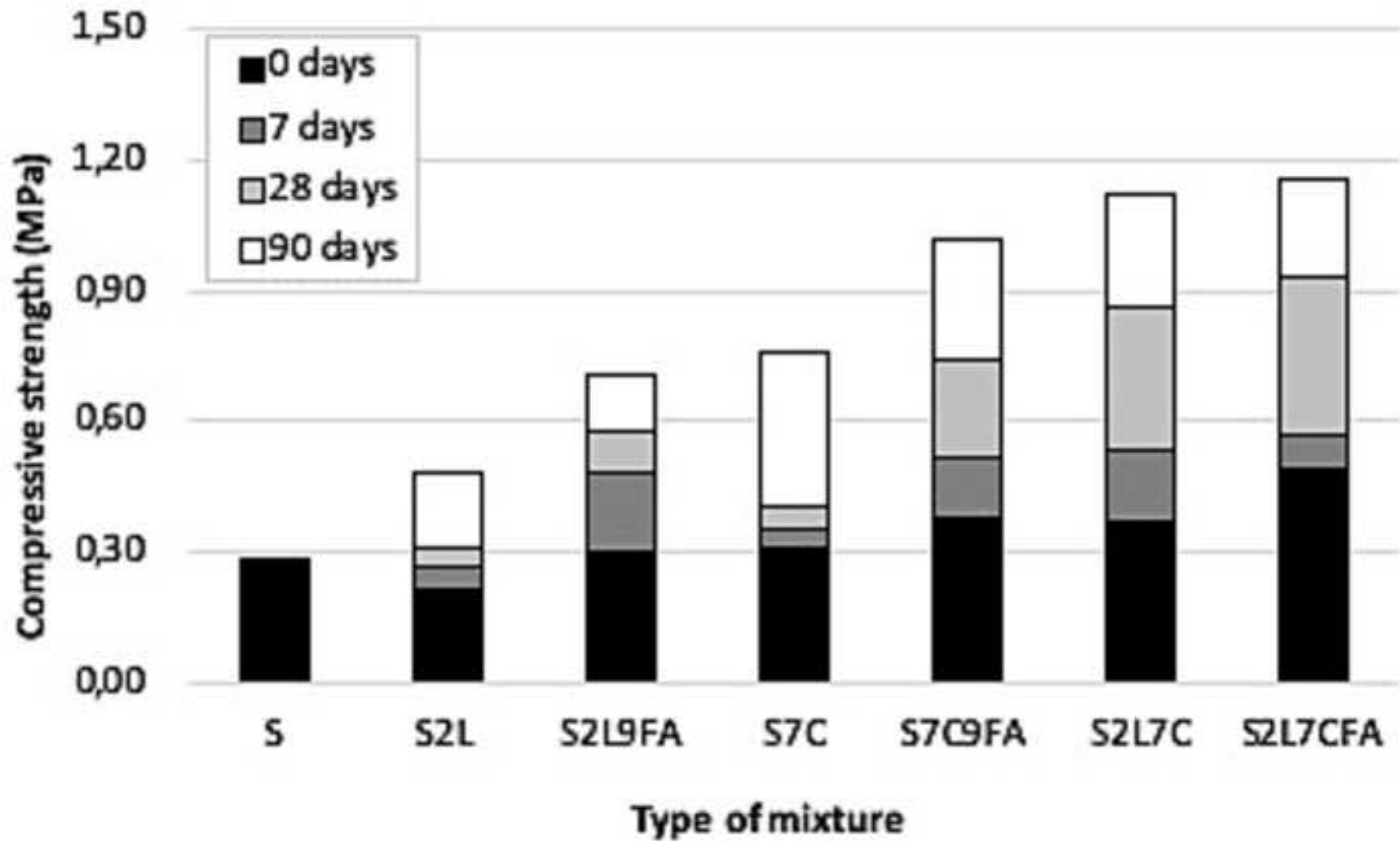


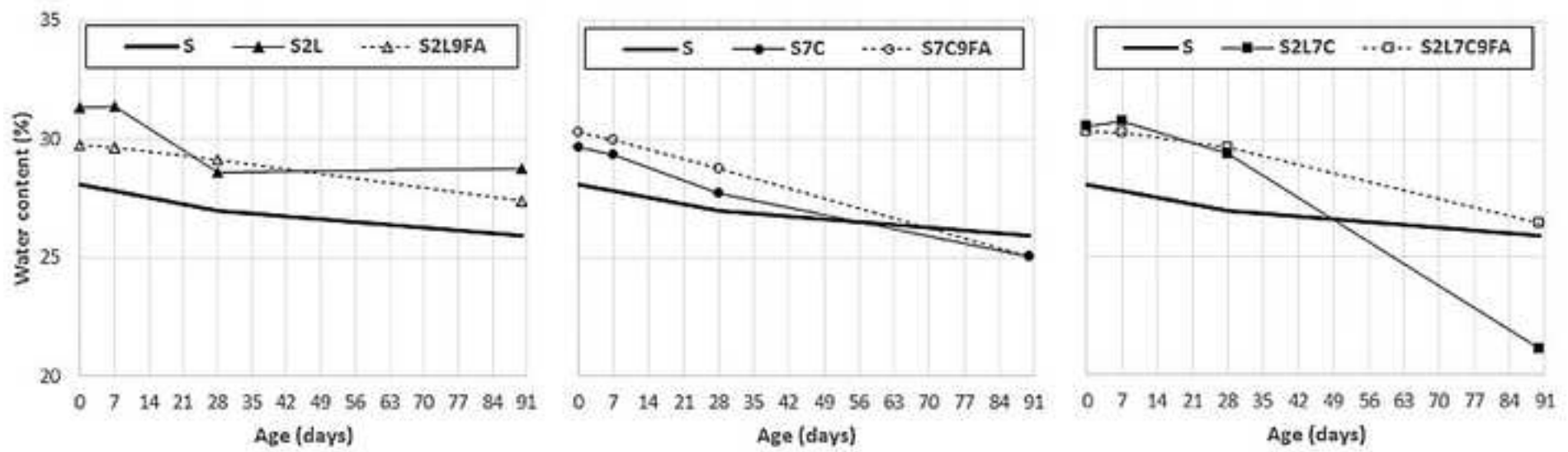
(b) mixtures with fly ash











# Effect of FA addition on microstructural and resistance characteristics of a stabilized soil using lime and cement

Ana Paula FURLAN, Andry RAZAKAMANANTSOA, Harifidy RANAIVOMANANA, Ouali AMIRI, Daniel LEVACHER, Dimitri DENELEE

## Graphic Abstract

